International Journal of Computer Applications Technology and Research
Volume 8–Issue 08, 299-302, 2019, ISSN:-2319–8656

An Enhanced Browser Reference Model

Harun Kamau
School of Computing and Informatics
Maseno University
Maseno, Kenya

Dr.O.McOyowo
School of Computing and Informatics
Maseno University,
Maseno, Kenya

Dr.O.Okoyo
School of Computing and Informatics
Maseno University,
Maseno, Kenya

Abstract: Browsers are prime software applications in modern computing devices. They are essential in accessing internet rich content. Access to these contents pose a high memory demand on the host device thus affecting the user browsing experience and running of other programs. The architectural model adopted by the current browsers lacks a memory control mechanism that would prevent memory hogging which results to device crawl. The paper critically addresses the weaknesses of the contemporary browser reference architecture with a view to controlling memory hogging by integrating a memory analyzer into existing architecture.

Keywords: Browser reference architecture, memory hogging, web browser

1. INTRODUCTION

The Internet is gradually becoming a requisite element of modern generation. It is heavily relied upon in education sector where teaching and learning methods have gone digital. Business transactions have been digitized to reflect global reach and improve efficiency. Moreover, social and communication activities are being performed in a manner that makes the world a global village (Sagar A. et al., 2010). A web browser is prime software while seeking to realize the mentioned activities. While efficiency and multiprogramming is desired in the target computing devices, memory becomes an impending factor in realizing state of art performances. Studies have shown that browsers are memory ravenous and their consumption is dynamic contrary to generic computer programs (Doug DePerry, 2012).

The architectural model has been established to be a contributing factor to memory hogging which to leads to a computer freeze (Kamau, 2018). Modern browsers including Mozilla Firefox, Chrome, and Internet Explorer are derived from the reference architecture postulated by Allan and Michael (2006). In this architectural model, the browser continuously requests memory from the operating system to load the content it has fetched. This phenomenon leads to memory hogging and thus reduces the degree of multiprogramming. In single-processor systems, this phenomenon is undesired. To avert this problem, modification of the current model becomes a necessity. This is done with a view to providing memory control mechanism that would limit the maximum amount of memory a browser can use. This prevents memory hogging and thus increases the level of multiprogramming.

1.1 Contemporary Model

The architecture constitutes five major modules, which include User interface, Browser engine, Rendering engine, Display backend and Data persistence. This model was derived by Allan and Michael in 2006. These modules work collaboratively to interpret intricate protocols and provide a visual display of the URL fetched, (Paulina Siva et al., 2016). Modules functionality is discussed in the subsections herein. An illustration of the interaction of the mentioned modules is as shown in figure 1.

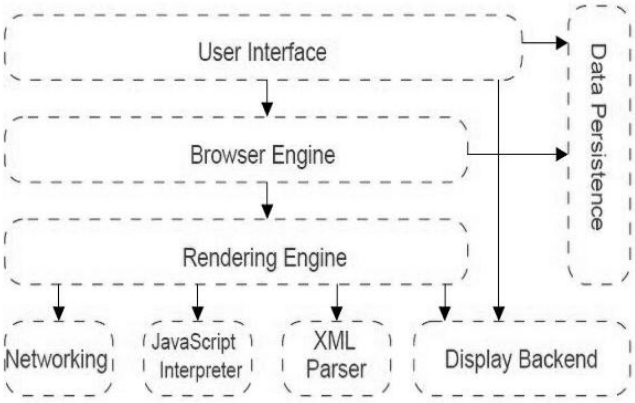

Figure 1:Browser reference architecture.

1.1.1User Interface

This module provides the methods with which a user interacts with the Browser Engine. It provides standard web browser

features including user preferences, printing functionality, downloading, opening and closing tabs etc. Browser designers have variant approaches in designing the user interface of the target browser. However, a given browser version depicts slight differences in user interface from another version of the same type. For instance, earlier versions of Mozilla Firefox had the reload button positioned to the right of the address bar while current versions have positioned to the left.

1.1.2 Browser Engine

This module provides a high-level interface to the Rendering Engine. It provides methods to initiate the loading of a URL and other high-level browsing actions like reload, back and forward. Furthermore, it provides the User interface with various messages relating to error messages and loading progress. When the browser fails to fetch the content specified by the URL, appropriate messages are conveyed to the User Interface, seeking intervention of the browser user.

1.1.3 Rendering Engine

This module provides the visual representation of the fetched URL. It comprises various subsystems that enable the browser to interpret the content of the URL. A URL contains two major parts: protocol and web resource. The protocol defines the mechanism through which resource will be fetched. Common protocols include HTTP and FTP. Web resources include text documents, images/graphics, audio and video. The multimedia content is interpreted by the appropriate parser to visually human-readable format. A prime component of the Rendering Engine is the HTML parser. The HTML parser is often tightly integrated with the rendering engine for performance reasons and can provide varying levels of support for broken or nonstandard HTML .It can display other types of data via plug-ins or extension; for example, displaying PDF documents using a PDF viewer plug-in. The rendering engine has XML parser sub system that parses XML data. The JavaScript content in the URL is interpreted by the JavaScript Interpreter. Detailed functionality of mentioned subsystems is discussed in sub sections below. Different browsers use different rendering engines: Internet Explorer uses Trident, Firefox uses Gecko, and Safari uses WebKit. Chrome and Opera (from version 15) use Blink, a fork of WebKit.

1.1.3.1 Networking Component

This component provides functionality to handle URLs retrieval using the common Internet protocols like HTTP and FTP. It handles all aspects of Internet communication and security; character set translations and Multi-Purpose Internet Mail Extensions (MIME) type resolution. This component may also implement a cache of retrieved documents to minimize network traffic

1.1.3.2 JavaScript Interpreter

This component executes the JavaScript code that is embedded in a URL. Results of the execution are passed to the Rendering Engine for display. The Rendering Engine may disable various actions based on user defined properties. Where the browser user has set JavaScript code to be disabled, the rendering engine ignores the interpreted material.

1.1.3.3 XML Parser

This is a software library or a package that provides an interface for client applications to work with XML documents. It is generic and reusable component with a standard that has well defined interface. It checks for proper format of the XML document and may also validate the XML documents. Modern day browsers have built-in XML parsers. The goal of a parser is to transform XML data into a human-readable code.

1.1.4 Display/UI Backend

This component is tightly coupled with the host operating system. It provides primitive drawing and windowing methods that are host operating system dependent. Common widgets like combo box, an input box, a check box, etc are drawn using UI properties.

1.1.5 Data Persistence

The Data Persistence component manages user's data such as bookmarks, cookies and preferences. The browser may need to save all sorts of data locally. Browsers also support storage mechanisms such as localStorage, IndexedDB, WebSQL and FileSystem (Michael Coates, 2010).

1.2 Flaws of the Current Browser Reference Architecture

The contemporary architecture has two main weaknesses which are outlined herein.

i. The rendering engine processes the requests made by the browser engine by rendering the fetched content provided there is little memory available for use by the browser. If the operating system can no longer allocate any more memory, the computer freezes hence becomes unusable.

ii. The browser process prevents other legitimate processes from being loaded in the main memory if it consumes almost all-available memory. This reduces the level of multiprogramming.

2. METHODS

The enhanced model was anchored on browser reference architecture highlighted in figure 1

2.1 Necessity to Modify Browser Reference Architecture

From the weaknesses highlighted in section 1.2, there was need to restructure the architecture to provide a control mechanism for browser memory usage. While seeking to address this problem, the researcher opted to integrate a memory analyzer to the contemporary browser reference architecture.

2.2 The Enhanced Browser Reference Architecture

The enhanced architecture incorporates the Memory Analyzer component as shown in figure 2. The memory analyzer component interacts with the operating system to track memory usage in real-time and to check browser memory consumption against the set threshold total memory. After analysis, the browser user is provided with possible actions to take to prevent memory hogging. Consequently, more applications can be loaded into the main memory awaiting execution. This guarantees that browsers do not make computer to freeze by delimiting other legitimate applications from running. As a result, it improves the level of multiprogramming and ultimately improves user-browsing experience. The analyzer is implemented as a software module included in the web browser application.

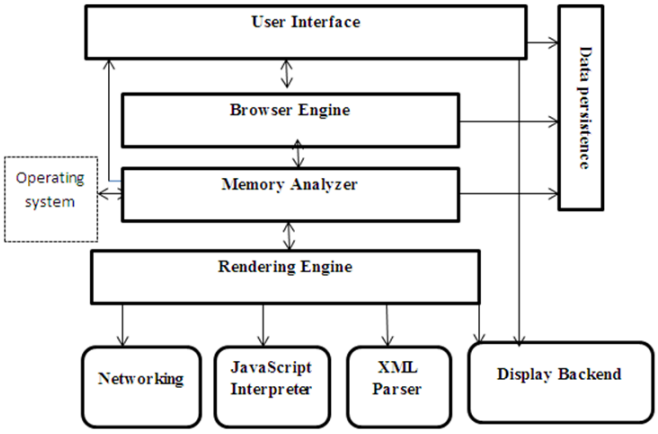

Figure 2: The enhanced browser reference architecture

2.2.1Memory Analyzer

This component checks real-time memory consumption for the browser against the threshold total memory limit set by the user and gives feedback information to the user on possible actions to take to prevent memory hogging by the browser. Memory analysis is done after the browser engine has retrieved a resource. The rendering engine interprets and gives a visual representation of the URL with the help of parsers and JavaScript interpreter if memory space is available. The integration provides memory control mechanism that hence controls memory hogging. Furthermore, the analyzer provides garbage collection mechanism to reclaim unused memory from the browser objects.

2.2.2 Flow diagram of memory analyzer

A conceptualized design of a Memory Analyzer and its interactions with other modules is as shown in figure 3. When a user enters a URL on the browser's address bar and hits the Go button, the Browser Engine takes the URL and attempts to fetch its content. The Memory Analyzer performs analysis of the memory consumed against the threshold memory as set by the user. If the memory is lower than the threshold memory, it passes the content of the URL to the rendering engine for further actions. However, if the consumed memory gets higher than the threshold memory, a notification error message is passed to the higher modules for action to be taken by the user.

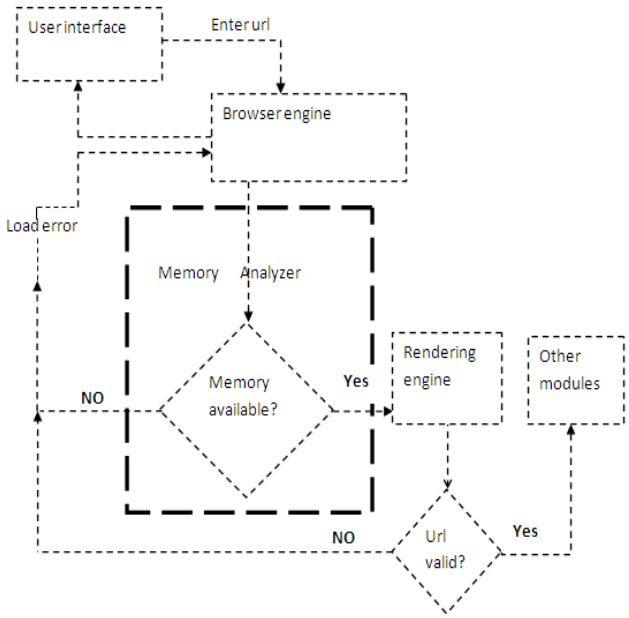

Figure 3: The Flow diagram of a memory analyzer

3. CONCLUSION

Based on the structure of the current browser architecture, it is evident enough that the model lacks a memory control mechanism and thus memory hogging becomes a habitual phenomenon in browser applications. In attempt to solve this problem, the memory analyzer was integrated to the current model with a view to providing memory control mechanism. Further, the module notifies the user when memory hogging is detected. The researcher designed a browser prototype and integrated the memory analyzer in it.

4. RECOMMENDATION

An evaluation of the enhanced browser reference should be done to unveil its performance with regard to memory consumption and its overall impact on user browsing experience.

5. REFERENCES

[1] A. E. Hassan and R. C. Holt, (2000). A reference architecture for web servers. In Proceedings of 7th the Working Conference on Reverse Engineering (WCRE ’00), pp. 150–160, 2000.

[2] A. Taivalsaari and T. Mikkonen, (2011). "The Web as an Application Platform: The Saga Continues," *Proc. 37th Euromicro Conf. Software Engineering and Advanced Applications* (SEAA 11), IEEE CS, 2011, pp. 170–174.

[3] A. Taivalsaari et al., (2008). Web Browser as an Application Platform: The Lively Kernel Experience, tech. report TR-2008-175, Sun Microsystems Labs, 2008.

[4] Accuvant Labs, 2011: Browser Security Comparison; A Quantitative Approach. Retrieved from http://files.accuvant.com/web/files/AccuvantBrowserSec C ompar_FINAL.pdf

[5] Alan Grosskurth and Michael W. Godfrey, (2005) Reference architecture for web browsers. In ICSM'05: Proceedings of the 21st IEEE International Conference on Software Maintenance (ICSM'05), pp 661-664, Washington, DC, USA, 2005. IEEE Computer Society.

[6] Alan Grosskurth, Michael W. Godfrey ,(2006) Architecture and evolution of the modern web browser. Retrieved from http://grosskurth.ca/papers/browser- archevol-20060619.pdf

[7] Allan Grosskurth and Michael Godfrey, (2014). Reference architecture for web browsers. In Journal of Software Maintenance and Evolution: Research and Practice, pp 1–7, 2006

[8] Chris Anderson (2012). The Man Who Makes the Future: Wired Icon Marc Andreessen. Retrieved from http://www.wired.com/2012/04/ff_andreessen/all/

[9] Doug Deperry, (2012). HTML5 security in the modern web browser perspective**.**

[10] Kamau, H.,McOyowo, S. & Okoyo, H. (2018): *Techniques to control memory hogging by web browsers.* International Journal of Computer Applications Technology and Research. Vol. 7 issue 04,2018

[11] Matthew Braga (2011): Web Browser Showdown: Memory Management Tested. Retrieved from http://www.tested.com/tech/web/2420-web-browser-showdown-memory-management-tested/index.php

[12] Michael Coates (2010). *A journey in Security*. HTML5, Local Storage, and XSS. Retrieved from http://michaelcoates.blogspot.com/2010/07/html5-local-storage-and-xss.html

[13] Paulina S., Raúl M., & Eduardo B. (2016). *A Reference Architecture for web browsers*: Part I, A pattern for Web Browser Communication

[14] Vrbanec, T., Kiric, N. & Varga, M. (2013). “The evolution of web browser architecture”. SCIECONF 2013, pp. 472–480.

[15] W3C (2004). Architecture of the World Wide Web, Volume one. Retrieved from http://www.w3.org/TR/webarch/

International Journal of Computer Applications Technology and Research
Volume 8–Issue 08, 303-310, 2019, ISSN:-2319–8656

Energy Estimates and Decay of Solutions to a Plate Equation with Memory

Yongqin Liu
School of Mathematics and Physics,
North China Electric Power University,
Beijing 102206, China

Jingjing Li
School of Mathematics and Physics,
North China Electric Power University,
Beijing 102206, China

Abstract: This paper focuses on the initial-value problem of a linear plate equation with memory in multi-dimensions ($n \geq 1$), the decay structure of which is of regularity-loss property. By making use of the point-wise estimate of solutions in the Fourier space, the energy estimates and decay estimates of solutions to the linear problem are obtained.

Keywords: plate equation with memory; point-wise estimate; decay estimates; energy estimates

2010 Mathematical Subject Classification Numbers:
35G10;35L30;35B40

1. INTRODUCTION

In this paper we consider the initial-value problem of the following linear plate equation with memory term in multi-dimensional space $\mathbb{R}^n$with n ≥ 1:

$$u_{tt} + \Delta^2 u - \Delta u + g * \Delta u = 0 \qquad (1.1)$$

with the initial data

$$u(x,0) = u_0(x), u_t(x,0) = u_1(x). \qquad (1.2)$$

Here $u = u(x,t)$ is the unknown function of $x = (x_1,\cdots,x_n) \in \mathbb{R}^n$ and $t > 0$, and represents the transversal displacement of the plate at the point x and the time t. The term $g * \Delta u = \int_0^t g\,(t-\tau)\Delta u(\tau)d\tau$ equivalent to the memory term and g satisfies:

Assumption [1]
1) $g \in C^2(\mathbb{R}^+) \cap W^{2,1}(\mathbb{R}^+)$,
2) $g(s) > 0,\ -C_0 g(s) \leq g'(s) \leq -C_1 g(s),$
$|g''(s)| \leq C_2 g(s),\ \forall s \in R^+,$
3) $1 - \int_0^t g\,(s)ds \geq C_3,\ \forall t \in \mathbb{R}^+,$
where $C_i (i = 1,2,3)$ are positive constants.

The inertial model of quasilinear dissipative plate equation, whose linear part is given by:

$$u_{tt} - \Delta u_{tt} + \Delta^2 u + u_t = 0. \qquad (1.3)$$

here $-\Delta u_{tt}$ corresponds to the rotational inertia and u_t is the linear dissipative term. In [1], Da-Luz and Charão studied a semi-linear dissipative plate equation (1.3). They proved the global existence of solutions and a polynomial decay of the energy by exploiting an energy method. However their result was restricted to the lower dimensional case $1 \leq n \leq 5$. This restriction on the space dimension was removed by Sugitani and Kawashima by making use of the sharp decay estimates for the equation (1.3) in [2]. In [3], Liu and Kawashima obtained the global existence and asymptotic behavior of solutions by employing the time-weighted energy method combined with a semi-group argument. In this paper the plate equation with memory (1.1) is also of regularity-loss property, just like the inertial model of dissipative plate equation (1.3) in [2, 3]. The decay structure of the regularity-loss is characterized by the property

$$\rho(\xi) = \frac{|\xi|^2}{(1+|\xi|^2)^2},$$

where $\rho(\xi)$ is introduced in the point-wise estimate in the Fourier space of solutions to the linear problem. It is evident that the decay structure is very weak in the higher-frequency domain since $\rho(\xi) \to 0$ as $\xi \to \infty$. The decay structure of the regularity-loss type was also observed in [4,5,6,7]. For more studies on various aspects of dissipation of plate equations, we refer to [8,9,10,11]. Also, as for the study of decay properties for hyperbolic systems of memory-type dissipation, we refer to [12,13,14,15,16].

The main aim of this paper is to study decay estimates of solutions to the initial value problem (1.1) and (1.2). Firstly, by using Fourier transform and Laplace transform, we obtain the solution u to the linear problem (1.1) and (1.2) given by (2.4) and the solution operators G(t)∗ and H(t)∗. Secondly, by employing the energy method in the Fourier space, we obtain the pointwise estimate in the Fourier space of solutions to the linear problem (1.1) and (1.2), appealing to which we obtain the point-wise of solution operators and their properties. Finally, the decay estimates of solutions to (1.1), (1.2) are achieved.

The contents of the paper are as follows. Solution formula are obtained in section 2. In section 3, we obtain the estimates and properties of solutions operators, which is based on the point-wise estimate in the Fourier space of solutions to the linear problem. In the last section, we prove the decay estimates of solutions to the linear problem by virtue of the properties of solution operator.

Before closing this section, we give some notations to be used below.

Let $\mathcal{F}[f]$ denote the Fourier transform of f defined by

$$\mathcal{F}[f] = \hat{f}(\xi) := \frac{1}{(2\pi)^{\frac{n}{2}}} \int_{\mathbb{R}^n} e^{-ix\cdot\xi} f(x)dx,$$

and we denote its inverse transform as $\mathcal{F}^{-1}$.

$L^p = L^p(\mathbb{R}^n)(1 \le p \le \infty)$ is the usual Lebesgue space with the norm $\|\cdot\|_{L^p}$. $W^{m,p}(\mathbb{R}^n)$, $m \in Z_+$, $p \in [1,\infty)$ denote the usual Sobolev space with its norm

$$\| f \|_{W^{m,p}} := (\sum_{k=0}^{m} \| \partial_x^k f \|_{L^p}^p)^{\frac{1}{p}}.$$

In particular, we use $W^{m,2} = H^m$. Here, for a nonnegative interger k, ∂_x^k denotes the totality or each of all the k-th order derivatives with respect to $x \in \mathbb{R}^n$. Also, $C^k(I; H^m(\mathbb{R}^n))$ denotes the space of k -times continuously differentiable functions on the interval I with values in the Sobolev space $H^m = H^m(\mathbb{R}^n)$.

Finally, in this paper, we denote every positive constant by the same symbol C or c without confusion. $[\cdot]$ is Gauss symbol.

2. Solution Formula

In this section, we try to obtain the solution formula for the problem (1.1) and (1.2). Assume that $G(x,t)$ and $H(x,t)$ are the solutions to the following problem:

$$\begin{cases} G_{tt} + \Delta^2 G - \Delta G + g * \Delta G = 0, \\ G(x,0) = \delta(x), \\ G_t(x,0) = 0. \end{cases} \quad (2.1)$$

$$\begin{cases} H_{tt} + \Delta^2 H - \Delta H + g * \Delta H = 0, \\ H(x,0) = 0, \\ H_t(x,0) = \delta(x). \end{cases} \quad (2.2)$$

Apply Fourier transform and Laplace transform to (2.1) and (2.2), then we can obtain $\hat{G}(\xi,t)$ and $\hat{H}(\xi,t)$.

Now we compute $\hat{G}(\xi,t)$, First, apply Fourier transform to (2.1), we can obtain the following equation:

$$\begin{cases} \hat{G}_{tt} + |\xi|^4 \hat{G} + |\xi|^2 \hat{G} - |\xi|^2 g * \hat{G} = 0, \\ \hat{G}(\xi,0) = \hat{\delta}(\xi) = C, \\ \hat{G}_t(\xi,0) = 0. \end{cases}$$

then apply Laplace transform to above equation, we can get

$$\int_0^\infty \hat{G}_{tt}\, e^{-\lambda t} dt + (|\xi|^2 + |\xi|^4) \int_0^\infty \hat{G}\, e^{-\lambda t} dt - |\xi|^2 \int_0^\infty (g * \hat{G}) e^{-\lambda t} dt = 0,$$

by computing, we have that

$$-C\lambda + (\lambda^2 + |\xi|^2 + |\xi|^4)\mathcal{L}[\hat{G}](\lambda) - |\xi|^2 \mathcal{L}[g](\lambda) \cdot \mathcal{L}[\hat{G}](\lambda) = 0,$$

So

$$\mathcal{L}[\hat{G}](\lambda) = \frac{C\lambda}{\lambda^2 + |\xi|^2 + |\xi|^4 - |\xi|^2 \mathcal{L}[g](\lambda)}$$

Similarly,

$$\mathcal{L}[\hat{H}](\lambda) = \frac{C}{\lambda^2 + |\xi|^2 + |\xi|^4 - |\xi|^2 \mathcal{L}[g](\lambda)}.$$

finally, we have formally that

$$\hat{G}(\xi,t) = C\mathcal{L}^{-1}[\frac{\lambda}{\lambda^2 + |\xi|^2 + |\xi|^4 - |\xi|^2 \mathcal{L}[g](\lambda)}](\xi,t),$$

$$\hat{H}(\xi,t) = C\mathcal{L}^{-1}[\frac{1}{\lambda^2 + |\xi|^2 + |\xi|^4 - |\xi|^2 \mathcal{L}[g](\lambda)}](\xi,t).$$

Here C is a constant determined by the initial data in (2.1) and (2.2).

Lemma 2.1. $\hat{G}(\xi,t)$ and $\hat{H}(\xi,t)$exist.

Proof. We only prove $\hat{G}(\xi,t)$exists; similarly we could prove $\hat{H}(\xi,t)$ exists. Denote $F(\lambda) := \lambda^2 + |\xi|^2 + |\xi|^4 - |\xi|^2 \mathcal{L}[g](\lambda)$. To prove$\mathcal{L}^{-1}[\frac{\lambda}{F(\lambda)}]$exists, we need to consider the zero points of $F(\lambda)$. Denote $\lambda = \sigma + i\nu$, $\sigma > -C_1$, C_1 is same as that in Assumption [1] 2), then $\mathcal{L}[g](\lambda)$ exists. Assume that $\lambda_1 = \sigma_1 + i\nu_1$ is a zero point of $F(\lambda)$ and $\sigma_1 > -C_1$, then σ_1 and ν_1 satisfy

$$\begin{cases} \mathrm{Re}F(\lambda_1) = \sigma_1^2 - \nu_1^2 + |\xi|^2 + |\xi|^4 - |\xi|^2 \int_0^\infty \cos(\nu_1 t) e^{-\sigma_1 t} g(t) dt = 0, \\ \mathrm{Im}F(\lambda_1) = 2\sigma_1\nu_1 + |\xi|^2 \int_0^\infty \sin(\nu_1 t) e^{-\sigma_1 t} g(t) dt = 0. \end{cases} \quad (2.3)$$

If $\xi = 0$, from(2.3), we know that $\sigma_1 = 0, \nu_1 = 0$.

If $\xi \neq 0$, we claim that $\sigma_1 < 0$. Now we prove the claim by contradiction.

Assume that $\sigma_1 \ge 0$. If $\nu_1 = 0$, then in view of $\int_0^\infty g(t)dt < 1$, we obtain that

$$\mathrm{Re}F(\lambda_1) = \sigma_1^2 + |\xi|^2 + |\xi|^4 - |\xi|^2 \int_0^\infty e^{-\sigma_1 t} g(t) dt > 0$$

it yields contradiction with$(2.3)_1$.

If $\nu_1 \neq 0$, then we have that

$$\mathrm{Im}F(\lambda_1) = \nu_1(2\sigma_1 + |\xi|^2 \int_0^\infty \frac{\sin(\nu_1 t)}{\nu_1} e^{-\sigma_1 t} g(t) dt).$$

Next we prove that $\int_0^\infty \frac{\sin(\nu_1 t)}{\nu_1} e^{-\sigma_1 t} g(t) dt > 0$. Denote $a_m = \int_0^{\frac{2m\pi}{|\nu_1|}} \frac{\sin|\nu_1 t|}{|\nu_1|} e^{-\sigma_1 t} g(t) dt$, and we will prove $\{a_m\}_{m=1}^\infty$ is a convergent sequence. By direct computation, we have that

$$a_1 = \int_0^{\frac{\pi}{|\nu_1|}} \frac{\sin|\nu_1 t|}{|\nu_1|} (e^{-\sigma_1 t} g(t) - e^{-\sigma_1 (t + \frac{\pi}{|\nu_1|})} g(t + \frac{\pi}{|\nu_1|})) dt.$$

Since $\partial_t(e^{-\sigma_1 t} g(t)) < 0$, we have that $0 < a_1 < \int_0^{\frac{\pi}{|\nu_1|}} t\, e^{-\sigma_1 t} g(t) dt$. Similarly,

$$a_{m+1} - a_m = \int_{\frac{2m\pi}{|\nu_1|}}^{\frac{2m\pi+\pi}{|\nu_1|}} \frac{\sin|\nu_1 t|}{|\nu_1|} (e^{-\sigma_1 t} g(t) - e^{-\sigma_1 (t + \frac{\pi}{|\nu_1|})} g(t + \frac{\pi}{|\nu_1|})) dt,$$

so we have that $0 < a_{m+1} - a_m < \int_{\frac{2m\pi}{|\nu_1|}}^{\frac{2m\pi+\pi}{|\nu_1|}} t\, e^{-\sigma_1 t} g(t) dt$.

It yields that

$$0 < a_m < \int_0^{\frac{2m\pi}{|\nu_1|}} t\, e^{-\sigma_1 t} g(t) dt \le \frac{g(0)}{(\sigma_1 + C_1)^2},$$

so $\{a_m\}_{m=1}^\infty$ is a bounded and monotonic increasing sequence. Since $a_1 > 0$, $a(\lambda_1) := \lim_{m\to\infty} a_m > 0$. Thus we proved that

$\int_0^\infty \frac{\sin|\nu_1 t|}{|\nu_1|} e^{-\sigma_1 t} g(t)dt > 0$. Also, because $\sigma_1 \geq 0, \xi \neq 0$ and $\nu_1 \neq 0$, it results that $\mathrm{Im}F(\lambda_1) \neq 0$. This contradicts with $(2.3)_2$. Thus by contradiction we proved the claim $\sigma_1 < 0$.

Combining the two cases, we know that $\frac{\lambda}{F(\lambda)}$ is analytic in $\{\lambda \in \mathbb{C}; \mathrm{Re}(\lambda) > 0\}$ if $\xi = 0$ and in $\{\lambda \in \mathbb{C}; Re(\lambda) \geq 0\}$ if $\xi \neq 0$. Take $\lambda = \sigma + i\nu, \sigma > \max\{\mathrm{Re}\lambda_s\}$, here $\{\lambda_s\}$ is the set of all the singular points of $F(\lambda)$, then we have that

$$\mathcal{L}^{-1}\left[\frac{\lambda}{F(\lambda)}\right](t) = \int_{\sigma-i\infty}^{\sigma+i\infty} \frac{\lambda e^{\lambda t}}{F(\lambda)} = \int_{-\infty}^{+\infty} \frac{i(\sigma+i\nu)e^{(\sigma+i\nu)t}}{F(\sigma+i\nu)} d\nu$$

$$= \int_{\{\nu;|\nu|\leq R\}} + \int_{\{\nu;|\nu|>R\}} =: J_1 + J_2$$

J_1 converges, so we only need to consider J_2. Notice that $\frac{\lambda}{F(\lambda)} = \frac{1}{\lambda} - \frac{|\xi|^2+|\xi|^4-|\xi|^2\mathcal{L}[g](\lambda)}{\lambda F(\lambda)}$ and $|\mathcal{L}[g](\lambda)| \leq C$, then it is not difficult to prove that J_2 converges. The constant C in the expression of $\hat{G}(\xi, t)$ is determined by the initial data of $G(x, t)$. So far we complete the proof.

In view of Lemma 2.1 and Duhamel principle, the solution to the problem (1.1) and (1.2) could be expressed as following:

$$u(t) = G(t) * u_0 + H(t) * u_1. \qquad (2.4)$$

3. Decay Properties of Solution Operators

In this section, our goal is to get the decay estimates of the solution operators $G(t)*$ and $H(t)*$in the solution formula (2.4).

Proposition 3.1. Let k and l be integers, $\varphi \in H^{s+1}(\mathbb{R}^n)\cap L^p(\mathbb{R}^n)$, $\psi \in H^{s-1}(\mathbb{R}^n)\cap L^p(\mathbb{R}^n)$, $1 \leq p \leq 2$, then the following estimates hold:

1) $\| \partial_x^k G(t) * \varphi \|_{L^2} \leq C(1+t)^{-\frac{k}{2}-\frac{n}{2}\left(\frac{1}{p}-\frac{1}{2}\right)} \| \varphi \|_{L^p}$
$+C(1+t)^{-\frac{l}{2}} \| \partial_x^{k+l} \varphi \|_{L^2}$,
for $k \geq 0, l \geq 0, l+k \leq s+1$.

2) $\| \partial_x^k G_t(t) * \varphi \|_{L^2} \leq C(1+t)^{-\frac{k+1}{2}-\frac{n}{2}\left(\frac{1}{p}-\frac{1}{2}\right)} \| \varphi \|_{L^p}$
$+C(1+t)^{-\frac{l}{2}} \| \partial_x^{k+l+2} \varphi \|_{L^2}$,for $k \geq 0$, $l \geq 0, l+k \leq s-1$.

3) $\| \partial_x^k H(t) * \psi \|_{L^2} \leq C(1+t)^{-\frac{k-1}{2}-\frac{n}{2}\left(\frac{1}{p}-\frac{1}{2}\right)} \| \psi \|_{L^p}$
$+C(1+t)^{-\frac{l+2}{2}} \| \partial_x^{k+l} \psi \|_{L^2}$,
for $k \geq 1, l+2 \geq 0, 0 \leq l+k \leq s-1$.

4) $\| \partial_x^k H_t(t) * \psi \|_{L^2} \leq C(1+t)^{-\frac{k}{2}-\frac{n}{2}\left(\frac{1}{p}-\frac{1}{2}\right)} \| \psi \|_{L^p}$
$+C(1+t)^{-\frac{l}{2}} \| \partial_x^{k+l} \psi \|_{L^2}$,
for $k \geq 0, l \geq 0, l+k \leq s-1$.

To prove proposition 3.1, the key point is to obtain the point-wise estimates of the fundamental solutions in the Fourier space. In fact this could be achieved by using the following point-wise estimate of solutions to the linear problem (1.1) and (1.2).

Lemma 3.1. Assume u is the solution of (1.1) and (1.2), then it satisfies the following point-wise estimate in the Fourier space:

$$|\hat{u}_t(\xi,t)|^2 + (|\xi|^2+|\xi|^4)|\hat{u}(\xi,t)|^2 + |\xi|^2(g\square\hat{u})(\xi,t) \leq Ce^{-C\rho(\xi)t}(|\hat{u}_1(\xi)|^2 + (|\xi|^2+|\xi|^4)|\hat{u}_0(\xi)|^2), \qquad (3.1)$$

here $\rho(\xi) = \frac{|\xi|^2}{(1+|\xi|^2)^2}$.

To prove Lemma 3.1, we denote some notations. For any real or complexvalued function $f(t)$, we define

$$(g*f)(t) := \int_0^t g(t-\tau)f(\tau)d\tau,$$
$$(g\diamond f)(t) := \int_0^t g(t-\tau)(f(\tau)-f(t))d\tau,$$
$$(g\square f)(t) := \int_0^t g(t-\tau)|f(t)-f(\tau)|^2 d\tau.$$

We have the following lemma rely on direct calculation, which is useful in obtaining our point-wise estimate of solution in the Fourier space.

Lemma 3.2. For any function $k \in C(\mathbb{R})$, and any $\phi \in W^{1,2}(0,T)$, it holds that

1) $(k*\phi)(t) = (k\diamond\phi)(t) + (\int_0^t k(\tau)d\tau)\phi(t)$,

2) $2Re\{(k*\phi)(t)\overline{\phi}_t(t)\} = -k(t)|\phi(t)|^2 + (k'\square\phi)(t) - \frac{d}{dt}\{(k\square\phi)(t) - (\int_0^t k(\tau)d\tau)|\phi(t)|^2\}$,

3) $|(k\diamond\phi)(t)|^2 \leq (\int_0^t |k(\tau)|d\tau)(|k|\square\phi)(t)$.

Next we will come to get the point-wise estimates of solutions to the problem (1.1), (1.2) in the Fourier space.

Proof of Lemma 3.1

Step 1: Apply Fourier transform to (1.1), we have that

$$\hat{u}_{tt} + (|\xi|^2+|\xi|^4)\hat{u} - |\xi|^2 g*\hat{u} = 0 \qquad (3.2)$$

By multiplying (3.2) by $\overline{\hat{u}}_t$ and taking the real part, we have that

$$\left\{\frac{1}{2}|\hat{u}_t|^2 + \frac{1}{2}(|\xi|^2+|\xi|^4)|\hat{u}|^2\right\}_t - |\xi|^2 Re\{g*\hat{u}\overline{\hat{u}}_t\} = 0. \qquad (3.3)$$

Use Lemma 3.2. 2) To the term $Re\{g*\hat{u}\overline{\hat{u}}_t\}$ in （3.3）, we have that

$$Re\{g*\hat{u}\overline{\hat{u}}_t\} = -\frac{1}{2}g(t)|\hat{u}|^2 + \frac{1}{2}(g'\square\hat{u})(t) - \frac{1}{2}\frac{d}{dt}\left\{(g\square\hat{u})(t) - \int_0^t g(\tau)d\tau|\hat{u}|^2\right\}.$$

We denote

$$E_1(\xi,t) = |\hat{u}_t|^2 + (|\xi|^2+|\xi|^4)|\hat{u}|^2 + |\xi|^2 g\square\hat{u} - |\xi|^2\left(\int_0^t g(s)ds\right)|\hat{u}|^2,$$
$$F_1(\xi,t) = |\xi|^2(g|\hat{u}|^2 - g'\square\hat{u}),$$

then we have that

$$\frac{\partial}{\partial t}E_1(\xi,t) + F_1(\xi,t) = 0. \qquad (3.4)$$

Step 2: By multiplying （3.2） by $\{-(g*\overline{\hat{u}})_t\}$ and taking the real part, we have that

$$\left\{\frac{1}{2}|\xi|^2|g*\hat{u}|^2\right\}_t - Re\{\hat{u}_{tt}(g*\overline{\hat{u}})_t\} -$$

$$Re\{(|\xi|^2+|\xi|^4)\hat{u}(g*\overline{\hat{u}})_t\}=0. \quad (3.5)$$

Since $(g*\overline{\hat{u}})_t = g(0)\overline{\hat{u}} + g'*\overline{\hat{u}}$, the second term in (3.5) yields that

$$\begin{aligned}-Re\{\hat{u}_{tt}(g*\overline{\hat{u}})_t\} &= -Re\{\hat{u}_t(g*\overline{\hat{u}})_t\}_t + Re\{\hat{u}_t(g*\overline{\hat{u}})_{tt}\}\\ &= -Re\{\hat{u}_t(g*\overline{\hat{u}})_t\}_t + Re\{\hat{u}_t(g(0)\overline{\hat{u}}_t + (g'*\overline{\hat{u}})_t)\}\\ &= -Re\{\hat{u}_t(g*\overline{\hat{u}})_t\}_t + Re\{g(0)|\hat{u}_t|^2 + \hat{u}_t(g'*\overline{\hat{u}})_t\}.\end{aligned}$$

We denote

$$E_2(\xi,t)=\frac{1}{2}|\xi|^2|g*\hat{u}|^2 - Re\{\hat{u}_t(g*\overline{\hat{u}})_t\},$$

$$F_2(\xi,t)=g(0)|\hat{u}_t|^2,$$

$$R_2(\xi,t)=Re\{-\hat{u}_t(g'*\overline{\hat{u}})_t + (|\xi|^2+|\xi|^4)\hat{u}(g*\overline{\hat{u}})_t\},$$

then obtain that

$$\frac{\partial}{\partial t}E_2(\xi,t)+F_2(\xi,t)=R_2(\xi,t). \quad (3.6)$$

Step 3: By multiplying (3.2) by $\overline{\hat{u}}$ and taking the real part, we have that

$$Re\{\hat{u}_t\overline{\hat{u}}\}_t - |\hat{u}_t|^2 + (|\xi|^2+|\xi|^4)|\hat{u}|^2 - |\xi|^2 Re\{g*\hat{u}\overline{\hat{u}}\}=0. \quad (3.7)$$

Due to Lemma 3.2 1), we obtain that

$$Re\{g*\hat{u}\overline{\hat{u}}\}=\left(\int_0^t g(s)ds\right)|\hat{u}|^2 + Re\{g\diamond\hat{u}\overline{\hat{u}}\}.$$

We denote

$$E_3(\xi,t)=Re\{\hat{u}_t\overline{\hat{u}}\},$$

$$F_3(\xi,t)=(|\xi|^2+|\xi|^4)|\hat{u}|^2 - |\xi|^2\left(\int_0^t g(s)ds\right)|\hat{u}|^2,$$

$$R_3(\xi,t)=|\hat{u}_t|^2+|\xi|^2 Re\{g\diamond\hat{u}\overline{\hat{u}}\},$$

Then (3.7) yields that

$$\frac{\partial}{\partial t}E_3(\xi,t)+F_3(\xi,t)=R_3(\xi,t). \quad (3.8)$$

Define $\rho(\xi)=\frac{|\xi|^2}{(1+|\xi|^2)^2}$, and denote

$$E(\xi,t)=E_1(\xi,t)+\rho(\xi)(\alpha E_2(\xi,t)+\beta E_3(\xi,t)),$$

$$F(\xi,t)=F_1(\xi,t)+\rho(\xi)(\alpha F_2(\xi,t)+\beta F_3(\xi,t)),$$

$$R(\xi,t)=\rho(\xi)(\alpha R_2(\xi,t)+\beta R_3(\xi,t)),$$

where α,β are positive constants, then (3.4), (3.6) and (3.8) yield that

$$\frac{\partial}{\partial t}E(\xi,t)+F(\xi,t)=R(\xi,t). \quad (3.9)$$

We introduce Lyapunov functions:

$$E_0(\xi,t)=|\hat{u}_t|^2+(|\xi|^2+|\xi|^4)|\hat{u}|^2+|\xi|^2 g\square\hat{u}.$$

$$F_0(\xi,t)=g\square\hat{u}+g|\hat{u}|^2.$$

By the definitions of $E_1(\xi,t)$ and $F_1(\xi,t)$, we know that there exist some positive constants c_i (i=1,2,3) such that the following inequalities hold:

$$c_1E_0(\xi,t)\le E_1(\xi,t)\le c_2E_0(\xi,t),\ F_1(\xi,t)\ge c_3|\xi|^2F_0(\xi,t). \quad (3.10)$$

On the other hand,

$$|E_2(\xi,t)|\le C|\hat{u}_t|^2+C(1+|\xi|^2)(|\hat{u}|^2+g\square\hat{u}),$$

$$|E_3(\xi,t)|\le C(|\hat{u}_t|^2+|\hat{u}|^2),$$

$$\begin{aligned}&\left|\rho(\xi)\big(\alpha E_2(\xi,t)+\beta E_3(\xi,t)\big)\right|\\ &\le C(\alpha+\beta)\{|\hat{u}_t|^2+|\xi|^2(|\hat{u}|^2+g\square\hat{u})\}\\ &\le c_4(\alpha+\beta)E_0(\xi,t).\end{aligned}$$

Choose α,β appropriately small such that $c_4(\alpha+\beta)\le min(\frac{c_1}{2},\frac{c_2}{2})$, from (3.10) we have that

$$\frac{c_1}{2}E_0(\xi,t)\le E(\xi,t)\le\frac{3c_2}{2}E_0(\xi,t). \quad (3.11)$$

In consideration of (3.10) and the fact that $0\le\int_0^t g(s)ds\le 1$, it is not difficult to verify that

$$F(\xi,t)\ge c_3|\xi|^2F_0(\xi,t)+\rho(\xi)\{\alpha g(0)|\hat{u}_t|^2+\beta|\xi|^4|\hat{u}|^2\}. \quad (3.12)$$

By virtue of Lemma 3.2 , we have that

$$\begin{aligned}|R_2(\xi,t)|\le{}&\varepsilon|\hat{u}_t|^2+\delta(|\xi|^2+|\xi|^4)|\hat{u}|^2\\ &+C_{\varepsilon,\delta}(|\xi|^2+|\xi|^4)F_0(\xi,t),\end{aligned}$$

and

$$|R_3(\xi,t)|\le|\hat{u}_t|^2+\gamma|\xi|^2|\hat{u}|^2+C_\gamma|\xi|^2 g\square\hat{u},$$

where $\varepsilon,\delta,\gamma$ are positive constants, we have

$$\begin{aligned}|R(\xi,t)| &\le\rho(\xi)\{(\alpha\varepsilon+\beta)|\hat{u}_t|^2+(\alpha\delta+\beta\gamma)(|\xi|^2+|\xi|^4)|\hat{u}|^2\\ &\quad+\alpha C_{\varepsilon,\delta}(|\xi|^2+|\xi|^4)F_0(\xi,t)+\beta C_\gamma|\xi|^2 g\square\hat{u}\}\\ &\le(\alpha\varepsilon+\beta)\rho(\xi)|\hat{u}_t|^2+(\alpha\delta+\beta\gamma)|\xi|^2|\hat{u}|^2+(\alpha+\beta)C_{\varepsilon,\delta,\gamma}|\xi|^2F_0(\xi,t).\end{aligned}$$

We claim that there exist $\gamma,\varepsilon,\delta,\alpha,\beta$ such that

$$|R(\xi,t)|\le\frac{1}{2}F(\xi,t). \quad (3.13)$$

First choose $\gamma=\frac{1}{4}$, $\varepsilon=\frac{1}{4}g(0)$, $\delta=\frac{1}{16}g(0)$, $\beta=\frac{1}{4}\alpha g(0)$, then the next three inequalities hold:

$$(\alpha+\beta)C_{\varepsilon,\delta,\gamma}\le\frac{1}{2}c_3,$$

$$\alpha\varepsilon+\beta\le\frac{1}{2}\alpha g(0),$$

$$\alpha\delta+\beta\gamma\le\frac{1}{2}\beta,$$

In order to certify (3.13) (here (3.11) is also considered), it suffices to choose α suitably small such that

$$\alpha+\beta=\left(1+\frac{1}{4}g(0)\right)\alpha\le min\{\frac{c_3}{2C_{\varepsilon,\delta,\gamma}},\frac{c_1}{2c_4},\frac{c_2}{2c_4}\}$$

Due to (3.9) and (3.13), we get that

$$\frac{\partial}{\partial t}E(\xi,t)+\frac{1}{2}F(\xi,t)\le 0. \quad (3.14)$$

On the other hand, due to (3.11) and (3.12) we obtain that

$$F(\xi,t)>c\rho(\xi)E(\xi,t). \quad (3.15)$$

From (3.14) and (3.15), we have that

$$E(\xi,t)\le e^{-c\rho(\xi)t}E(\xi,0). \quad (3.16)$$

By virtue of (3.11) and (3.16), we have that

$$|\hat{u}_t|^2+(|\xi|^2+|\xi|^4)|\hat{u}|^2+|\xi|^2 g\square\hat{u}\le$$

$$Ce^{-C\rho(\xi)t}(|\hat{u}_1(\xi)|^2 + (|\xi|^2 + |\xi|^4)|\hat{u}_0(\xi)|^2),$$

so, we obtain the point-wise estimates of solutions to (1.1), (1.2) in the Fourier space.

As a simple corollary of Lemma 3.1, we have the following point-wise estimates of the fundamental solutions $G(x,t)$ and $H(x,t)$ in the Fourier space.

Lemma 3.3. $G(x,t)$ and $H(x,t)$ satisfy

1) $|\hat{G}(\xi,t)| \le Ce^{-C\rho(\xi)t}$,

2) $|\hat{G}_t(\xi,t)| \le Ce^{-C\rho(\xi)t}(|\xi|^2 + |\xi|^4)^{\frac{1}{2}}$,

3) $|\hat{H}(\xi,t)| \le Ce^{-C\rho(\xi)t}(|\xi|^2 + |\xi|^4)^{-\frac{1}{2}}$,

4) $|\hat{H}_t(\xi,t)| \le Ce^{-C\rho(\xi)t}$,

where $\rho(\xi) = \frac{|\xi|^2}{(1+|\xi|^2)^2}$.

Proof. Putting (2.4) with $u_1 = 0$ in (3.1), it results that

$$|\hat{G}_t(\xi,t)|^2 + (|\xi|^2 + |\xi|^4)|\hat{G}(\xi,t)|^2 \le Ce^{-C\rho(\xi)t}(|\xi|^2 + |\xi|^4).$$

It yields 1) and 2) of Lemma 3.3.

Putting (2.4) with $u_0 = 0$ in (3.1), it results that

$$|\hat{H}_t(\xi,t)|^2 + (|\xi|^2 + |\xi|^4)|\hat{H}(\xi,t)|^2 \le Ce^{-C\rho(\xi)t}.$$

It yields 3) and 4) of Lemma 3.3. □

Now we use Lemma 3.3 to prove Proposition 3.1.

Proof of Proposition 3.1. In view of Lemma 3.3 1), we have that

$$\begin{aligned} \| \partial_x^k G_t(t) * \varphi \|_{L^2}^2 &\le C\int_{R^n} |\xi|^{2k} e^{-C\rho(\xi)t} |\hat{\varphi}(\xi)|^2 d\xi \\ &\le C\int_{\{\xi:|\xi|\le 1\}} |\xi|^{2k} e^{-\frac{C}{4}|\xi|^2 t} |\hat{\varphi}|^2 d\xi + C\int_{\{\xi:|\xi|\ge 1\}} |\xi|^{2k} e^{-\frac{Ct}{4|\xi|^2}} |\hat{\varphi}(\xi)|^2 d\xi \\ &\le C(1+t)^{-n(\frac{1}{p}-\frac{1}{2})-k} \| \varphi \|_{Lp}^2 + C(1+t)^{-l} \| \partial_x^{k+l} \varphi \|_{L^2}^2, \end{aligned}$$

here $k \ge 0$, $l \ge 0$, $l + k \le s + 1$. Thus 1) is proved.

Due to Lemma 3.3 2) , it results that

$$\begin{aligned} \| \partial_x^k G_t(t) * \varphi \|_{L^2}^2 &\le C\int_{R^n} |\xi|^{2k} (|\xi|^2 + |\xi|^4) e^{-C\rho(\xi)t} |\hat{\varphi}(\xi)|^2 d\xi \\ &\le C\int_{\{\xi:|\xi|\le 1\}} |\xi|^{2k+2} e^{-\frac{C}{4}|\xi|^2 t} |\hat{\varphi}(\xi)|^2 d\xi + C\int_{\{\xi:|\xi|\ge 1\}} |\xi|^{2k+4} e^{-\frac{Ct}{4|\xi|^2}} |\hat{\varphi}(\xi)|^2 d\xi \\ &\le C(1+t)^{-n(\frac{1}{p}-\frac{1}{2})-k-1} \| \varphi \|_{Lp}^2 + C(1+t)^{-l} \| \partial_x^{k+l+2} \varphi \|_{L^2}^2, \end{aligned}$$

here $k + 1 \ge 0$, $l \ge 0$, $k + l + 2 \le s + 1$. Thus 2) is proved.

Next we prove 3) and 4). It follows from Lemma 3.3 3) that

$$\begin{aligned} \| \partial_x^k H(t) * \psi \|^2 &\le C\int_{R^n} |\xi|^{2k} (|\xi|^2 + |\xi|^4)^{-1} e^{-C\rho(\xi)t} |\hat{\psi}(\xi)|^2 d\xi \\ &\le C\int_{\{\xi:|\xi|\le 1\}} |\xi|^{2k-2} e^{-\frac{C}{4}|\xi|^2 t} |\hat{\psi}(\xi)|^2 d\xi + C\int_{\{\xi:|\xi|\ge 1\}} |\xi|^{2k} |\xi|^{-4} e^{-\frac{Ct}{4|\xi|^2}} |\hat{\psi}(\xi)|^2 d\xi \\ &\le C(1+t)^{-n(\frac{1}{p}-\frac{1}{2})-k+1} \| \psi \|_{Lp}^2 + C(1+t)^{-l-2} \| \partial_x^{k+l} \psi \|_{L^2}^2, \end{aligned}$$

here $k \ge 1$, $l \ge -2$, $0 \le k + l \le s - 1$. Thus 3) is proved.

Lemma 3.3 2) , yields that

$$\begin{aligned} \| \partial_x^k H_t(t) * \psi \|^2 &\le C\int_{R^n} |\xi|^{2k} e^{-C\rho(\xi)t} |\hat{\psi}(\xi)|^2 d\xi \\ &\le C(1+t)^{-n(\frac{1}{p}-\frac{1}{2})-k} \| \psi \|_{Lp}^2 + C(1+t)^{-l} \| \partial_x^{k+l} \psi \|_{L^2}^2, \end{aligned}$$

here $k \ge 0$, $l \ge 0$, $k + l \le s - 1$. thus 4) is proved.

4. Decay Estimates for Linear Problem.

In this section we study the decay estimates of solutions to the linear problem (1.1) and (1.2).

Theorem 4.1. *Let $s \ge 1$ be an integer. Assume that $u_0 \in H^{s+1}(\mathbb{R}^n)$ and $u_1 \in H^{s-1}(\mathbb{R}^n)$, and put*

$$I_0 = \| u_0 \|_{H^{s+1}} + \| u_1 \|_{H^{s-1}}.$$

Then the solution u to the problem (1.1) and (1.2) given by (2.4) satisfies

$$\partial_x u \in C^0([0,\infty)); H^s(\mathbb{R}^n)); u \in C^1([0,\infty); H^{s-1}(\mathbb{R}^n))$$

and the following energy estimate:

$$\| u_t(t) \|_{H^{s-1}}^2 + \| \partial_x u \|_{H^s}^2 + \int_0^t \| \partial_x u_t(\tau) \|_{H^{s-3}}^2 + \| \partial_x^2 u(\tau) \|_{H^{s-2}}^2 \, d\tau \le CI_0^2.$$

Proof. We have obtained the solution u of (1.1) and (1.2) given by (2.4) and proved that it satisfies the point-wise estimate (3.1) in the Fourier space.

From (3.14) and (3.15) we have that

$$\frac{\partial}{\partial t} E(\xi,t) + C\rho(\xi)E(\xi,t) \le 0.$$

Integrate the inequality with respect to t and appeal to （3.11）, then we obtain

$$E_0(\xi,t) + \int_0^t \rho(\xi) E_0(\xi,\tau) d\tau \le CE_0(\xi,t). \qquad (4.1)$$

Multiply (4.1) by $(1 + |\xi|^2)^{s-1}$ and integrate the resulting inequality with respect to $\xi \in \mathbb{R}^n$, then we have that

$$\| u_t(t) \|_{H^{s-1}}^2 + \| \partial_x u \|_{H^s}^2 + \int_0^t \| \partial_x u_t(\tau) \|_{H^{s-3}}^2 + \| \partial_x^2 u(\tau) \|_{H^{s-2}}^2 \, d\tau \le CI_0^2. \qquad (4.2)$$

(4.2) guarantees the regularity of the solution (2.4). So far we complete the proof of Theorem 4.1.

By using Proposition 3.1 with $p = 2$, we obtain the following decay estimate of u given by （2.4）, if initial data $u_0 \in H^{s+1}(\mathbb{R}^n)$ and $u_1 \in H^{s-1}(\mathbb{R}^n)$.

Theorem 4.2. Under the same assumption as in Theorem 4.1, then u given by (2.4) satisfies the decay estimate:

$$\| \partial_x^k u(t) \|_{H^{s+2-2k}} \le CI_0(1+k)^{-\frac{k-1}{2}}, 1 \le k \le [\frac{s+2}{2}]. \qquad (4.3)$$

Proof. Let $k \ge 1$, $m \ge 0$ be integers, In view of (2.4), by using 1) and 3) of Proposition 3.1 with $p = 2$, we have that

$$\left\| \partial_x^{k+m} u(t) \right\| \le \left\| \partial_x^{k+m} G(t) * u_0 \right\|_{L^2} + \left\| \partial_x^{k+m} H(t) * u_1 \right\|_{L^2}$$

$$\le C(1+t)^{-\frac{k+m}{2}-\frac{n}{2}\left(\frac{1}{p}-\frac{1}{2}\right)}\|u_0\|_{L^2}$$
$$+C(1+t)^{-\frac{l_1}{2}}\left\|\partial_x^{k+m+l_1}u_0\right\|_{L^2}$$
$$+C(1+t)^{-\frac{k-1+m}{2}-\frac{n}{2}\left(\frac{1}{p}-\frac{1}{2}\right)}\|u_1\|_{L^2}$$
$$+C(1+t)^{-\frac{l_2+2}{2}}\left\|\partial_x^{k+m+l_2}u_1\right\|_{L^2}$$
$$\le C(1+t)^{-\frac{k}{2}}\|u_0\|_{L^2}$$
$$+C(1+t)^{-\frac{k-1}{2}}\|u_1\|_{L^2}$$
$$+C(1+t)^{-\frac{l_1}{2}}\left\|\partial_x^{k+m+l_1}u_0\right\|_{L^2}$$
$$+C(1+t)^{-\frac{l_2+2}{2}}\left\|\partial_x^{k+m+l_2}u_1\right\|_{L^2}$$
$$\le C(1+t)^{-\frac{l_1}{2}}\left\|\partial_x^{k+m+l_1}u_0\right\|_{L^2}$$
$$+C(1+t)^{-\frac{l_2+2}{2}}\left\|\partial_x^{k+m+l_2}u_1\right\|_{L^2}$$
$$+C(1+t)^{-\frac{k-1}{2}}\|(u_0,u_1)\|_{L^2}$$

here $k\ge 1$, $k+m+l_1\le s+1$, $k+m+l_2\le s-1$. Choose the minimal integers l_1 and l_2 satisfying

$$\frac{l_1}{2}\ge\frac{k-1}{2},\ \frac{l_2+2}{2}\ge\frac{k-1}{2},$$

i.e. $l_1=k+1, l_2=l_1-2$, Then we obtain that

$$\|\partial_x^{k+m}u(t)\|_{L^2}\le CI_0(1+t)^{-\frac{k-1}{2}},$$

with $0\le m\le s+2-2k$. Take sum with $0\le m\le s+2-2k$, we obtain （4.3）. Thus Theorem （4.2） is proved.

Remark 4.1. Under the same assumption as in Theorem 4.1, u given by (2.4) also satisfies the following decay estimate:

$$\|\partial_x^k u_t(t)\|_{H^{s-1-2k}}\le CI_0(1+k)^{-\frac{k}{2}}, 0\le k\le[\tfrac{s-1}{2}].\ (4.4)$$

If we assume the initial data belong to $L^1(\mathbb{R})$, then by using Proposition （3.1） with $p=1$, we have the following sharp decay estimates.

Theorem 4.3. Let $s\ge 1$ be an integer. Assume that $u_0\in H^{s+1}(\mathbb{R}^n)\cap L^1(\mathbb{R}^n)$ and $u_1\in H^{s-1}(\mathbb{R}^n)\cap L^1(\mathbb{R}^n)$, and put

$$I_1=\|u_0\|_{H^{s+1}}+\|u_1\|_{H^{s-1}}+\|(u_0,u_1)\|_{L^1}.$$

Then the solution u to (1.1) and (1.2) given by (2.4) satisfies the following decay estimates:

$$\|\partial_x^k u(t)\|_{H^{s+2-2k-[\frac{n+1}{2}]}}\le CI_1(1+t)^{-\frac{k-1}{2}-\frac{n}{4}}, k\ge 1.\ (4.5)$$

Proof. Let $k\ge 1, m\ge 0$ be integers, In view of （2.4）, by using 1) and 3) of Proposition 3.1 with $p=1$, we have that

$$\left\|\partial_x^{k+m}u(t)\right\|\le\left\|\partial_x^{k+m}G(t)*u_0\right\|_{L^2}+\left\|\partial_x^{k+m}H(t)*u_1\right\|_{L^2}$$
$$\le C(1+t)^{-\frac{k+m}{2}-\frac{n}{2}\left(\frac{1}{p}-\frac{1}{2}\right)}\|u_0\|_{L^2}$$
$$+C(1+t)^{-\frac{l_1}{2}}\left\|\partial_x^{k+m+l_1}u_0\right\|_{L^2}$$
$$+C(1+t)^{-\frac{k-1+m}{2}-\frac{n}{2}\left(\frac{1}{p}-\frac{1}{2}\right)}\|u_1\|_{L^2}$$
$$+C(1+t)^{-\frac{l_2+2}{2}}\left\|\partial_x^{k+m+l_2}u_1\right\|_{L^2}$$
$$\le C(1+t)^{-\frac{k}{2}-\frac{n}{4}}\|u_0\|_{L^2}$$
$$+C(1+t)^{-\frac{k-1}{2}-\frac{n}{4}}\|u_1\|_{L^2}$$
$$+C(1+t)^{-\frac{l_1}{2}}\left\|\partial_x^{k+m+l_1}u_0\right\|_{L^2}$$
$$+C(1+t)^{-\frac{l_2+2}{2}}\left\|\partial_x^{k+m+l_2}u_1\right\|_{L^2}$$
$$\le C(1+t)^{-\frac{l_1}{2}}\left\|\partial_x^{k+m+l_1}u_0\right\|_{L^2}$$
$$+C(1+t)^{-\frac{l_2+2}{2}}\left\|\partial_x^{k+m+l_2}u_1\right\|_{L^2}$$
$$+C(1+t)^{-\frac{k-1}{2}-\frac{n}{4}}\|(u_0,u_1)\|_{L^2}$$

here $l_1\ge 0, l_2\ge -2, k+m+l_1\le s+1, 0\le k+m+l_2\le s-1$.
Choose the smallest integers l_1 and l_2 satisfying

$$\frac{l_1}{2}\ge\frac{k-1}{2}+\frac{n}{4},\ \frac{l_2+2}{2}\ge\frac{k-1}{2}+\frac{n}{4},$$

It yield that $l_1=k-1+[\frac{n+1}{2}]$, $l_2=l_1-2$. Thus m satisfies $0\le m\le s+2-2k-[\frac{n+1}{2}]$. Take sum with $0\le m\le s+2-2k-[\frac{n+1}{2}]$, we obtain that

$$\|\partial_x^k u(t)\|_{H^{s+2-2k-[\frac{n+1}{2}]}}\le CI_1(1+t)^{-\frac{k-1}{2}-\frac{n}{4}}, k\ge 1.$$

Thus Theorem 4.3 is proved.

Remark 4.2. Apart from the above decay estimates, by similar computation we also have the following estimate :

$$\|\partial_x^k u_t(t)\|_{H^{s-1-2k-[\frac{n+1}{2}]}}\le CI_1(1+t)^{-\frac{k}{2}-\frac{n}{4}}, k\ge 0.$$

Remark 4.3. The estimates in Theorem 4.2 and Theorem 4.3 indicate that the decay structure of solutions to the linear problem (1.1), (1.2) is of regularityloss type.

Acknowledgments

This work is partially supported by the Fundamental Research Funds for the Central Universities (Grant No. 2018MS052).

5. REFERENCES

[1] C. R. da Luz and R. C. Charão, Asymptotic properties for a semi-linear plate equation in unbounded domains, J. Hyperbolic Differential Equations, 6 (2009), 269-294.

[2] Y. Sugitani and S. Kawashima, Decay estimates of solutions to a semilinear dissipative plate equation, J. Hyperbol. Di. Eq., **7**(2010), 471-501.

[3] Y. Liu and S. Kawashima, Global existence and asymptotic behavior of solutions for quasi-linear dissipative plate equation, Discrete Contin. Dyn. Syst., 29 (2011), 1113-1139.

[4] Y. Liu and S. Kawashima, Decay property for a plate equation with memory-type dissipation, Kinet. Relat. Mod., 4 (2011), 531-547.

[5] Y. Liu and S. Kawashima, Global existence and decay of solutions for a quasi-linear dissipative plate equation, J. Hyperbol. Differ. Eq., 8 (2011), 591-614.

[6] T. Hosono and S. Kawashima, Decay property of regularity-loss type and application to some nonlinear hyperbolicCelliptic system, Math. Models Meth. Appl. Sci.,16 (2006), 1839-1859.

[7] K. Ide and S. Kawashima. Decay property of regularity-loss type and nonlinear effects for dissipative timoshenko system, Math. Models Meth. Appl. Sci., 18 (2008),1001-1025.

[8] Y. Liu, The pointwise estimates of solutions for semilinear dissipative wave equation, Commun. Pur. Appl. Anal., 12 (2013), 237-252.

[9] K. Nishihara, L^p–L^q estimates of solutions to the damped wave equation in 3-dimensional space and their application, Math. Z., 244 (2003), 631649.

[10] K. Nishihara and H.-J. Zhao, Decay properties of solutions to the Cauchy problem for the damped wave equation with absorption, J. Math. Anal. Appl., 313 (2006), 598–610.

[11] W. Wang and T. Yang, The pointwise estimates of solutions for Euler equations with damping in multi-dimensions, J. Differential Equations, 173 (2001), 410-450.

[12] P. M. N. Dharmawardane, J. E. Muñoz Rivera and S. Kawashima, Decay property for second order hyperbolic systems of viscoelastic materials, J. Math. Anal. Appl., 366 (2010), 621-635.

[13] M. Fabrizio and B. Lazzari, On the existence and the asymptotic stability of solutions for linear viscoelastic solids, Arch. Rational Mech. Anal., 116 (1991), 139-152.

[14] Y. Liu and S. Kawashima, Decay property for the Timoshenko system with memory-type dissipation, Math. Models Meth. Appl. Sci., 22 (2012), 1-19.

[15] Y. Liu and S. Kawashima, Global existence and asymptotic decay of solutions to the nonlinear Timoshenko system with memory, Nonlinear Analysis-TMA, 84 (2013), 1-17.

[16] J. E. Muñoz Rivera, M.G. Naso and F.M. Vegni, Asymptotic behavior of the energy for a class of weakly dissipative second-order systems with memory, J. Math. Anal. Appl.,286 (2003), 692-704.

International Journal of Computer Applications Technology and Research
Volume 8–Issue 08, 311-314, 2019, ISSN:-2319–8656

Broadband 5G Millimeter Wave Microstrip Antenna Design

Meng Li
School of Communication Engineering,
Chengdu University of Information Technology ,
Chengdu, China

Abstract: This paper presents an ultra-wideband microstrip antenna that can be used in the 5G millimeter wave band. Compared with similar literature, by rational use of the meandering technique, can effectively guarantee bandwidth. The size of the antenna is 18 mm × 28 mm × 0.514 mm. The return loss of the antenna reached 16.84% (26.93-31.89 GHz), which is higher than 15.7% of the similar literature and has a wider bandwidth. And the gain of the antenna is 9.21dBi, which is higher than 8.38dBi of the similar literature. Meet the efficiency requirements of 5G millimeter wave mobile communication systems.

Keywords: Broadband, 5G millimeter wave, Microstrip antenna, Size, Mobile communication

1. INTRODUCTION

Due to its thin profile, easy to conformal, low cost, and multi-polarization and multi-band operation, the microstrip antenna is widely used in various military and civilian communications and other fields[1]. However, the inherent narrow band and relative size of the microstrip antenna is 1/2 wavelength, which are it main shortcomings and the main factors restricting its development[2]. Therefore, expanding the frequency band of the microstrip antenna has become an important research field in wireless communication technology[3]. Researchers have proposed various structures to try to increase the bandwidth of microstrip antennas[4]. For example, a wide-band microstrip antenna with an H-shaped slot, a bidirectional antenna with a L-shaped slot, a millimeter-wave direction with a H-shaped slot coupled with a circularly polarized microstrip antenna , three-feed circular polarization Microstrip antenna, improved quasi-Yagi antenna, etc[5][6]. In 2015, Han Dongfang and others designed an antenna for 5G mobile communication. The working frequency band covers 27.3GHz-32.95GHz, the relative bandwidth is 15.7%, and the gain is the maximum gain of 8.38dBi in this band. In this paper, the improved structure of the antenna is studied, and the inverted "W" shape structure is added on the basis of the antenna. The return loss of the antenna in the band 26.93-31.89 GHz is less than -10 dB, which increases the relative bandwidth while increasing the radiation gain of the antenna, so that the gain reaches 9.20 dBi.

2. ANTENNA STRUCTURE DESIGN

Figure 1 shows the general shape of a broadband 5G millimeter wave microstrip antenna. The antenna consists of a ground plane, a radiating patch, a dielectric substrate, and a microstrip feed. The substrate material is Rogers RT / Duroid 5880（h = 0.17mm, =2.2, tan = 0.0009） Radiation antenna patch etched on top of the dielectric board, The patch adopts a symmetrical structure, and adopts a meandering technique to design the microstrip antenna into a petal shape and is dug with a 'W' shaped groove. The remaining sides of the groove are composed of a plurality of circular arcs, and current flows through the curved microstrip surface to increase the effective length of the antenna increases the resonance frequency point, and when a plurality of resonance frequency points are close, it can expand the bandwidth , and achieve the antenna is miniaturized. And there are 3 pairs of rectangular grooves on both sides of the patch to change the current on the surface of the patch to adjust the radiation characteristics. And the feeding with the progressive semicircular structure can effectively improve the radiation performance of the antenna. Only the radius is optimized, and the impedance matching of the antenna can be obtained, which reduces the design difficulty of the antenna. Similarly, the sides of the substrate are replaced by curved corners to facilitate the miniaturization of the antenna.

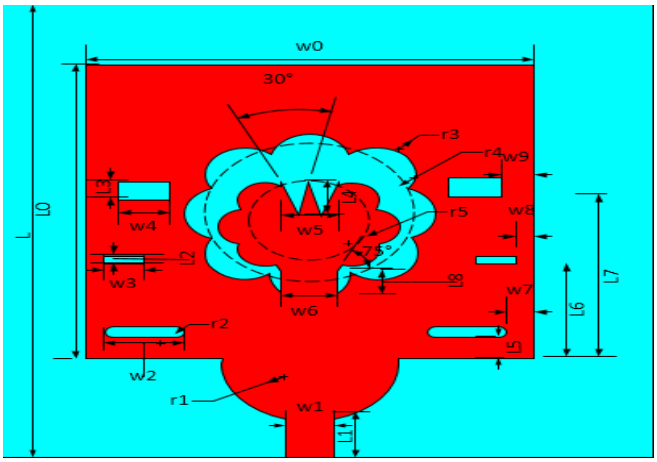

Figure.1. Shape of a broadband 5G millimeter wave microstrip antenna

3. THE MICROSTRIP SIZE

3.1 General microstrip antenna

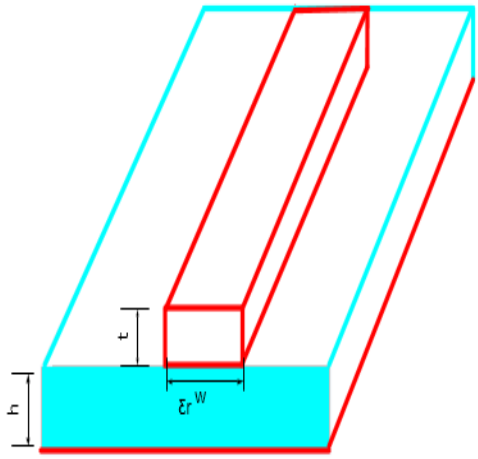

（a） Microstrip lne

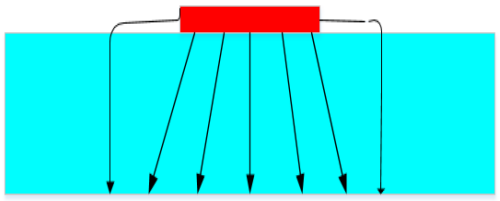

(b) Electric field lnes

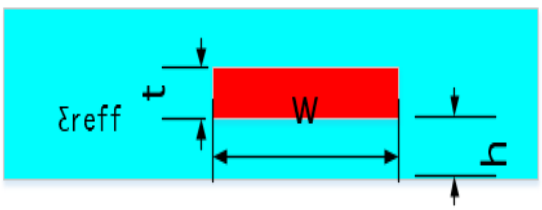

(c) Effective dielectric constant

Figure.2.General microstrip antenna

The microstrip line has a width W, a thickness t, a medium height h, and a dielectric constant. At the lateral edge of the microstrip line, a portion of the power line is in the air, and most of the power line is in the medium. As shown in Figure (b). Therefore, the microstrip line transmits a quasi-TEM mode. When W/h>>1 and >>1, the power line will mainly concentrate on the dielectric substrate, and the edge effect of the microstrip line is weakened, and the microstrip line is flat. Waveguide conversion, usually introducing an effective dielectric constant to describe the edge effect of the transverse field of the microstrip,As shown in (c), the microstrip line maintains the same electrical characteristics (propagation constant and characteristic impedance) at this time. There is $1<\varepsilon_{reff}<\varepsilon_r$,when there is air above the medium, And when $\varepsilon_r >>1$, ε_{reff} will be close to ε_r and will approach when $\varepsilon_r >>1$. ε_{reff} is also a function of frequency, and has a static value when the frequency is not high.

$$\varepsilon_{reff} = \frac{\varepsilon_r + 1}{2} + \frac{\varepsilon_r - 1}{2}[1+12\frac{h}{w}]^{-1/2}$$

$$\frac{w}{h} > 1$$

Due to the longitudinal edge effect, the electrical dimensions of the microstrip patch are larger than the actual physical size, as shown in Figure 3.

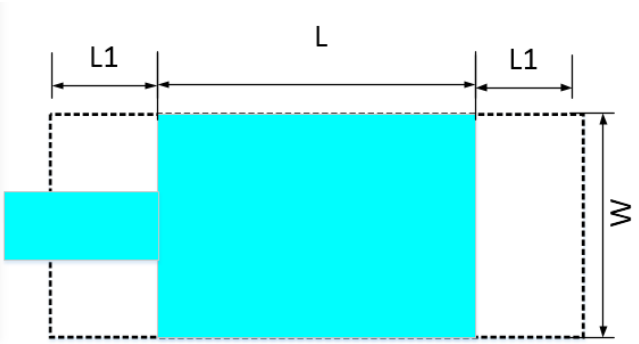

（a） Top view

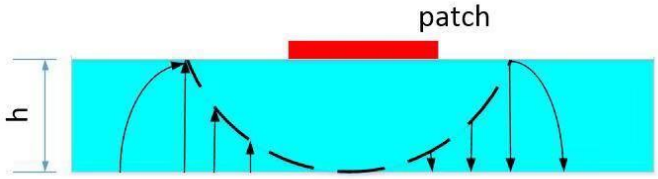

（b） side view

Figure.3.Edge effect

At both ends of the patch length direction, due to the fringe field effect, the two ends each extend in length L1, so for the main mode TM mode, the effective length:

$$L_{reff} = L + 2*L1$$

When the edge effect is not considered, the resonant frequency of the microstrip patch is:

$$(f_r)_{010} = \frac{1}{2*L\sqrt{\varepsilon_r}\sqrt{\mu_0\varepsilon_0}} = \frac{C_0}{2*L\sqrt{\varepsilon_r}}$$

C_0 is the free space speed of light.

When considering the edge effect, the microstrip patch resonant frequency is:

$$(f_{reff})_{010} = \frac{1}{2L_{reff}\sqrt{\varepsilon_r}\sqrt{\mu_0\varepsilon_0}} = \frac{1}{2(L+2L1)\sqrt{\varepsilon_{reff}}\sqrt{\mu_0\varepsilon_0}}$$

$q = \frac{(f_{rc})_{010}}{(f_r)_{010}}$ is called the edge factor. When the height of the medium increases, the edge effect is enhanced, the effective length is lengthened, the distance of the radiation groove is closer, and the resonant frequency of the patch is lowered.

3.2 Radiation patch design steps for microstrip patch antennas

Ple Given a dielectric substrate (ε_r , h) and frequency f_r , find W、L.

Step 1: to make the microstrip patch a good radiator, requires:

$$W = \frac{1}{2*f_r\sqrt{\mu_0\varepsilon_0}}\sqrt{\frac{2}{\varepsilon_r+1}} = \frac{C}{2f_r}\sqrt{\frac{2}{\varepsilon_r+1}}$$ Step 2: Calculate ε_{reff} according to the above analysis formula.

Step 3: Calculate L1 by the same reason.

Step 4: Calculate the actual patch length L:

$$L = \frac{1}{2*f_r\sqrt{\varepsilon_{reff}}\sqrt{\mu_0\varepsilon_0}} - 2L1$$

The antenna is designed and optimized using HFSS. The optimized antenna size is as follows:

Table 1. Antenna parameter table (unit:mm)

Table 1. Antenna parameter table (unit:mm)

variable	length	variable	length	variable	length
L	18	L0		r1	2.1
w0	18	L1	2.8	r2	0.15
w1	1	L2	0.3	r3	1.35
w2		L3	0.6	r4	3.36
w3	1	L4	2.02	r5	2.02
w4	1	L5		w7	4.2
w5	1.6	L6		w8	3.5
w6	1	L7		w9	4.2
L8	1.3				

4. ELECTROMAHNETIC SUMULATION AND RESULT ANALYSIS OF ANTENNA

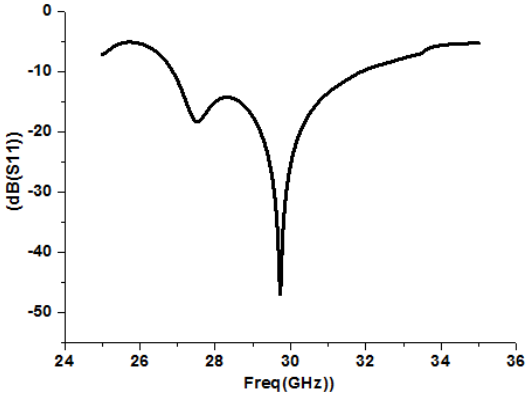

Figure.4. Echo Loss of Antenna

As can be seen from Figure x and Figure y, we achieved a wide bandwidth (16.84%) in the 5G FR2 band from 27.3GHz to 32.95GHz, which is higher than the similar literature and meets the requirements of the millimeter band. The maximum measurement gain of the antenna is 9.21 dBi, which is higher than the gain in the general literature. The size is only 18 mm × 28 mm × 0.514 mm, and the miniaturization of the broadband is also realized.

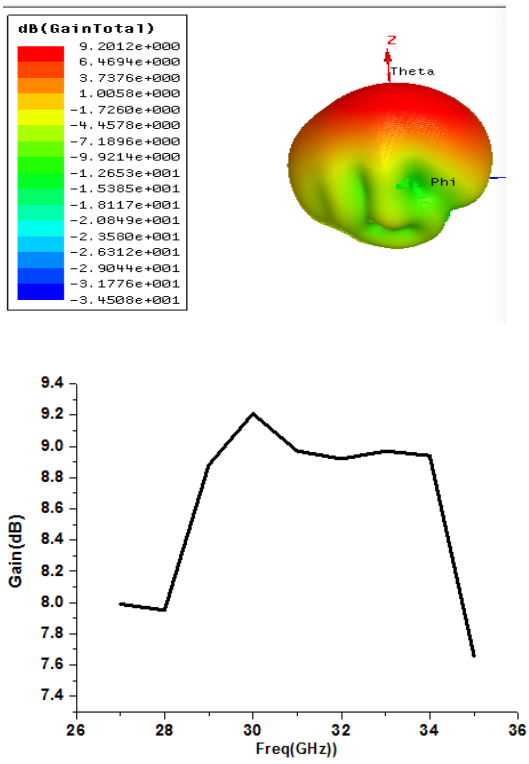

Figure.5. Gain of Antenna

5. CONCLUSION

This paper proposes a microstrip antenna with a wider bandwidth, working with the 5G millimeter wave band, which achieves 16.84% bandwidth by changing the antenna layout and semi-circular progressive feed. The antenna size is 18 mm × 28 mm × 0.514 mm. The slot structure in the antenna extends the bandwidth of the antenna by extending the length of the current propagation. The antenna achieves higher gain in the same literature and has a wider bandwidth, and can be used in a 5G mobile communication system and other wireless communication systems in a frequency band, and has high engineering practical value.

6. REFERENCES

[1] Targonski, S. D. , R. B. Waterhouse , and D. M. Pozar . "Design of wide-band aperture-stacked patch microstrip antennas." IEEE Transactions on Antennas and Propagation46.9(1998):1245-1251.

[2] Yang, Wanchen , W. Che , and H. Wang . "High-Gain Design of a Patch Antenna Using Stub-Loaded Artificial Magnetic Conductor." IEEE Antennas and Wireless Propagation Letters12(2013):1172-1175.

[3] Qian, Yongxi , et al. "A uniplanar quasi-Yagi antenna with wide bandwidth and low mutual coupling characteristics." IEEE Antennas and Propagation Society International Symposium. 1999 Digest. Held in conjunction with: USNC/URSI National Radio Science Meeting (Cat. No.99CH37010) IEEE, 2002.

[4] Wu, Chen . "A suspended microstripline-fed K-band linear-tapered slot antenna element and its 4 × 4 array designed by the finite-difference time-domain method." Microwave & Optical Technology Letters 51.10(2010):2406-2410.

[5] Yoshimura, Y. "A Microstripline Slot Antenna (Short Papers)." IEEE Transactions on Microwave Theory & Techniques 20.11(1972):760-762.

[6] Jang, Yong Woong . "A broadband cross-shaped microstripline-fed no-offset ring slot antenna." Microwave & Optical Technology Letters 36.1(2003):61-63.

International Journal of Computer Applications Technology and Research
Volume 8–Issue 08, 315-318, 2019, ISSN:-2319–8656

Improved device for particle concentration detection based on laser scattering and microscopic amplification

Li Na
Chengdu University of Information Technology
Institute of Communication Engineering
Chengdu, China

Xiong Rong
Chengdu University of Information Technology
Institute of Communication Engineering
Chengdu, China

Wen Bin
Chengdu University of Information Technology
Institute of Communication Engineering
Chengdu, China,

Abstract: With the rapid development of science and technology and industry, the formation of haze has been accelerated. Haze seriously harms our living environment and people's physical and mental health. Among them, atmospheric particulate pollution is the most serious environmental pollution at present. Therefore, timely and effective measures should be taken to detect atmospheric particulates in the environment, and then prevention and treatment of haze can effectively improve the environmental quality. Therefore, this paper designs an improved device for particle concentration detection based on laser scattering and micro-amplification, which is based on the previous designed concentration detection device. This device takes Mie scattering as the theoretical basis. The light source is a semiconductor laser, and the scattered light generated by the light irradiation of particles is further analyzed to obtain the particle property information after amplification by the microscopic equipment. At the same time, the photoelectric sensor absorbs the scattered light, and finally the particle mass concentration is reflected by pulse signal and optical signal together. There are two improvements in this device: 1. The structure of the stray light absorption part is modified to make more accurate measurement of experimental results and reduce the influence of stray light on the whole experiment; 2. Combined with image processing, the morphological features of particles can be acquired more accurately.

Keywords: Laser scattering; Microscopic magnification; Particle concentration detection; The image processing

1. INTRODUCTION

Particles refer to solid powder, liquid and gas with particle size less than 1mm.Particle size distribution and particle size are the main parameters to characterize the properties of particles, so it is of great significance to accurately measure particle size distribution and particle size [1]. The traditional particle detection methods include screening method, filter membrane weighing method [2], sedimentation method, electric induction method and piezoelectric crystal method [3]. Each measurement method has its own advantages and disadvantages. Traditional detection methods use large instruments, which are not convenient for real-time online measurement. However, some foreign laser particle size meters are very expensive and not easy to use on a large scale. Therefore, it is necessary to develop a small size, low cost and high precision particle concentration detection device.

The detection device designed in this paper adopts the method of light scattering [4-6] combined with microscopic amplification. When the incident light irradiates the particles, it will generate scattered light around, because the polarization degree and spatial distribution of scattered light are closely related to the particle size. By measuring these characteristic parameters, the particle size distribution and particle size of measured particles can be obtained. In order to observe the morphological characteristics of particulate matter more intuitively, this device combines the microscopic technology. Traditional microscopes can directly obtain the morphological characteristics of individual particles, but the volume of traditional microscopes is too large to meet the design requirements. This device improves the traditional microscope and realizes the design requirement of small size. But combined with the light scattering method, the stray light is treated. In general, the device designed in this paper can meet the requirements in terms of accuracy and stability, accurately measure the concentration of particles in the atmosphere, and realize real-time detection of the concentration of particles.

2. RELATED WORK

An improved device for particle concentration detection based on laser scattering and microscopic amplification is designed in this paper. In the design process, in order to ensure that each module can meet the application standards of the system, the function of each module is tested experimentally. Then, each module is combined into the final particle concentration detection device, which is used to measure the environmental particles in real time and analyze the measured data. Finally, compared with the measurement results of the particle concentration detector designed by PAN TENG Company, the performance of the device was evaluated. This paper mainly includes the following contents:

- Improvement of the structure of the microscopic device;

- Design of laser scattering device;

- Improvement of light absorption unit improves the absorption efficiency of stray light;

- Image processing and analysis of micro-enlarged images;

- Processing optical signals obtained by photoelectric sensors

Finally, the obtained photometric values and calculated pulse signals are analyzed and processed to deduce the mass concentration of particles.

3. FRAMEWORK

The improved device based on laser scattering and microscopic amplification is mainly used to measure the concentration of particles and directly observe the morphological characteristics of particles. Compared with the traditional indirect observation, this device adopts the direct observation method to conduct qualitative and quantitative research on the particles. Figure 1 shows the overall design of

the system, which consists of six parts, including particle detection device, CCD sensor [7], photodiode, amplifier circuit, A/D conversion circuit and PC.

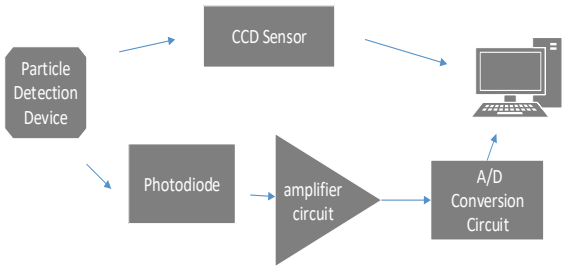

Figure. 1 Overall design of the system

As shown in the above, particle detection device respectively by CCD sensor and photoelectric diode will receive optical signals, and statistical analysis of the pulse signal to upload to PC photodiode will be collected by amplifying circuit to enlarge the weak signal processing, in order to facilitate the experimental calculation, will need to get to the analog signal into digital signal, through A/D conversion circuit to realize the transformation [8]. After data filtering, calculation and table lookup, data information of measured particles will be displayed on PC terminal. Combined with the optical signal obtained by CCD sensor through microscopic amplification, the concentration information of measured particles is obtained.

3.1 Structural improvement of microscopic devices

Special treatment was made on the structure of the microscope tube. The modified structure of the mirror tube was only about 2cm, so the whole microscope device has the characteristics of small size, easy to carry and accurate observation value. The design changes parts of the microscope tube to reduce its size, allowing it to be completely contained in a small box. By using the reflection principle of prism [9], the image transmitted from the objective lens can be seen completely and the focal length can be adjusted to obtain a clear and complete particle image for easy observation and counting. The specific design scheme of the whole device is shown in figure 2.

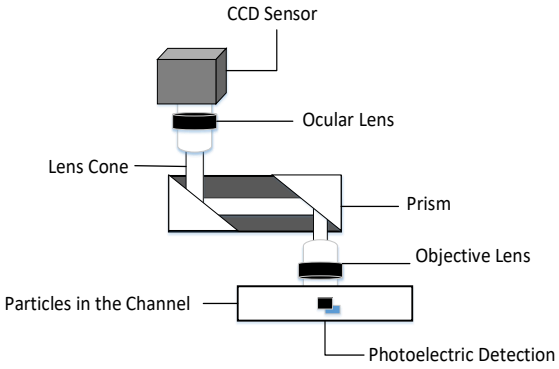

Figure. 2 Structure improvement of the microscopic device

3.2 Structure design of laser scattering device

3.2.1 Laser scattering device before improvement

The particle concentration detection device before improvement is shown in figure 3.According to the particle size measured by the device, the semiconductor laser [10] with the wavelength of 650nm is finally selected. The reason for choosing the semiconductor laser is that it has low cost compared with He-Ne laser [11] and has uniform light intensity in the photosensitive region compared with white light source. The laser passes through the collimator and the focusing lens through the sample pool, which is pumped through a device that allows particles to pass freely through the cavity. The photodiode connected to the focusing mirror and the diaphragm receives the scattered light generated by the particle, and then the photodiode gets the concentration information of the measured particle through amplification and analog-to-digital conversion. The acquisition device, which consists of a microscope and CCD sensor, allows researchers to see the light and shadow information left by particles passing through the particle cavity directly through the PC. The CCD captures the enlarged particle image, and then gets more accurate data through image processing.

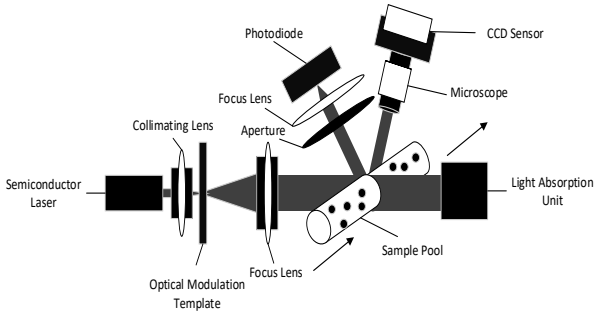

Figure. 3 Laser scattering device before improvement

3.2.2 Improved laser scattering device

For example, the detection device designed in the figure above is not very efficient in absorbing stray light in the light absorption unit, and the noise signal generated has a great influence on the experiment [12]. Therefore, the light absorption unit was improved, and the structure of the light absorption unit was designed into a spiral structure. Stray light can be ignored after several reflections, which improves the accuracy of the experiment. The improved laser scattering device is shown in figure 4.

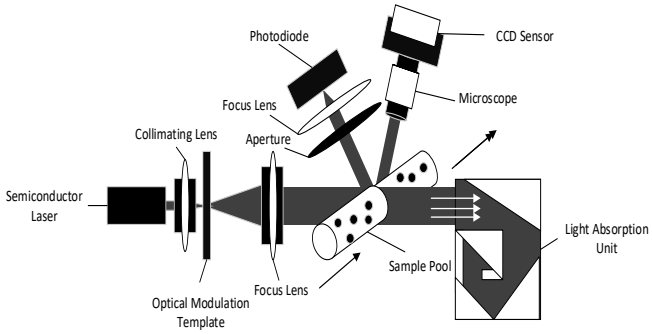

Figure. 4 Improved laser scattering device

3.3 Visual Angle recognition algorithm

As can be seen from the above figure, the collection device design of special micro-camera and laser instrument captures clear and enlarged particle images, and then gets more accurate data through image processing [13]. Therefore, the amplification multiple and precision of the collection device directly affect the accuracy of experimental results. Microscopic amplification design is adopted to amplify the particle signal. Image analysis method is adopted to

distinguish the size and properties of particles by combining the reflection of camera exposure rate, particle motion rate, particle size and other characteristics on the image. For the same particle, different wind speed and exposure time will affect the length of particle shadow. For different particles, under the same wind speed and exposure time, particle size will directly affect the width of particle shadow and the smoothness of surface. Therefore, in conclusion, the length (P_L), width (P_W) and smoothness (P_S) of particle shadow are directly related to particle velocity (V_P), camera exposure time (t) and particle morphology.

When the same particles pass through the particle cavity, the exposure time of the camera is fixed, only the wind speed is changed. When wind speed gradually increases, the length of particle drag shadow also increases, so the length of particle drag shadow is proportional to the speed of particle motion, that is, $P_L \propto V_P$. When the same particles pass through the particle cavity, the fixed wind speed only changes the exposure time of the camera. When the exposure time of the camera gradually increases, the length of particle drag shadow decreases, so the length of particle drag shadow is inversely proportional to the exposure time of the camera, that is, $P_L \propto \frac{1}{t}$.

In summary, if the particle is moving at a faster speed, a slightly increased camera exposure rate will yield a clear image. If the particles aren't moving fast, the camera shouldn't be exposed too fast. That is, the particles move faster and faster, and the corresponding camera exposure time gradually increases.

When different kinds of smooth particles pass through the particle cavity, the size of the fixed wind speed and the exposure time of the camera, the smoothness of the particle shadow only depends on the flatness of the particle itself.

Define the particle as a_i on each scale from left to right of its transverse width and a_j on each scale from bottom to top of its vertical height, then the relation between the width of particle shadow P_W and the width of particle W and the height of particle H is as follows.

$$P_W = \frac{\min(W,H)}{\max(W,H)} \qquad (1)$$

$W = \max(a_i) - \min(a_i)$, $H = \max(a_j) - \min(a_j)$. That is, when the particle is of slender length, P_W is the smallest. And vice versa.

4. EXPERIMENT

If the influence of background noise on experimental results can be reduced by improving the device, and the visual observation of experimental results can prove the stability and practicability of the device, then the concentration measurement of particulate matter will be more accurate.

4.1 Experiment preparation and setup

The particle concentration range used in this experiment is 40mg/m^3~1400 mg/m^3. According to the concentration range, several samples are extracted with concentrations of 40 mg/m^3, 100 mg/m^3, 300 mg/m^3, 400 mg/m^3, 570 mg/m^3, 780 mg/m^3 and 1336 mg/m^3 respectively.

4.2 Comparison of experimental results

Figure 1. Due to its vulnerability to the influence of tiny particles in the air, this experiment was conducted in a completely closed test chamber. In order to verify the accuracy of the experimental results, the concentration detector of PAN TENG Company was used as the standard to measure the particulate matter with different concentrations. Because the signal collected by photodiode will have the background noise caused by stray light and electrical noise. Before the addition of the improved light absorption device, due to the low concentration of particulate matter and the influence of noise, the photodiode receives very few scattered light signals. As shown in figure 5, the comparison between the measurement results and those of PAN TENG concentration meter is not ideal.

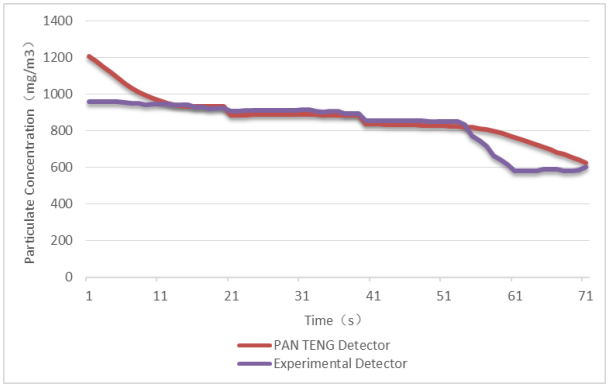

Figure. 5 Experimental results of noise effect

The experimental results of the improved over-light absorption device are shown in figure 6. The results of the improved experimental instrument are basically consistent with that of the climbing detector. Therefore, the improved experimental device in this paper can be fully applied in industry and meet the requirements of low cost and high precision.

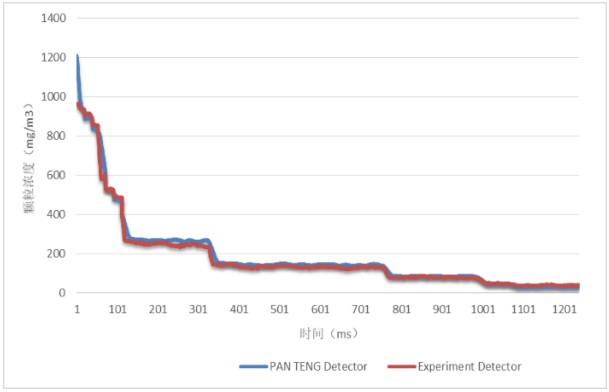

Figure. 6 Improved experimental results

4.3 Experimental results of image processing

The experimental results were simulated by Matlab. When a large number of flue gas particles passed through the particle cavity, the CCD sensor connected to the microscope equipment quickly photographed the particles directly below the microscope equipment in a short time, and then transmitted the acquired images to the computer for image processing. Figure 4.1 and figure 4.2 are images after grayscale and binarization processing. The size and

distribution of particles can be seen more clearly after image processing.

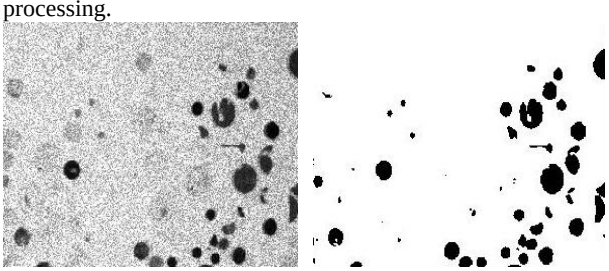

Figure. 7.1 Grayscale processed image
Figure 7.2 Binarization image

5. CONCLUSION

In this paper, an improved device for particle concentration detection based on laser scattering and microscopic amplification is designed. Based on the scattering signal of particles, the pulse signal and optical signal are used to invert the particle mass concentration. The improvement of light absorption unit greatly reduces the influence of noise signal on the experimental results, and the combination of image processing technology makes the experimental results more accurate. Through comparison and analysis with the concentration detector of PAN TENG Company, the device designed in this paper can meet the requirements in terms of accuracy and stability, accurately measure the concentration of particulate matter in the atmosphere, and make a certain contribution to environmental protection.

6. ACKNOWLEDGMENTS

First of all, I would like to thank my research tutor for his guidance, who pointed out the problems existing in the paper for me. Secondly, Xiong Rong helped me to successfully complete the measurement of the experimental results. I really thank them for helping me to finish this paper successfully.

7. REFERENCES

[1] MICHAEL B, CABMEN A, TERESA I F, et al. Air pollution and retained particles in the lung [J]. Environmental Health Perspectives, 2001, 109 (10):1039-1043.

[2] Feng J, Han P. Automatic monitoring instrument for atmospheric particulate matter based on filter membrane weighing method [J]. Computer and modernization, 2013(07):94-97+134.

[3] Chen S. Determination of airborne dust concentration by quartz piezoelectric crystal [J]. Environmental science and technology, 1985(01):19-20.

[4] Zhang S. Study on measurement technology of exhaust particulate matter based on light scattering principle [J]. Computer and digital engineering, 2019, 47(05):1254-1257+1263.

[5] Zhang Y. Research progress of PM2.5 detection technology [J]. Sensor world, 2019, 25(03):13-16.

[6] Zhou X. Performance comparison and optimization of PM2.5 sensor by light scattering method [J]. Journal of environment and health, 2016, 33(8): 739-743.

[7] Shen P. Design of linear CCD image acquisition and processing system based on FPGA [D]. Hubei University of technology, 2017.

[8] Jiang y, Zhou H, Zhan X. Circuit design of a dual-pole analog signal A/D conversion of single-chip microcomputer [J]. Electronic science and technology, 2014, 27(04):121-123.

[9] Gao Y, Sheng C, Liu Y. Study on phase diagram for measuring refractive index of prism by total reflection method [J]. College physics experiment, 2019, 32(02):34-36.

[10] Liu Z. Response characteristics of semiconductor laser and photodetector [D]. Xi 'an university of technology, 2019.

[11] Zuo C, Zhang X, Chen B, Wang C, Wang L. Study and design of light intensity of he-ne laser irradiated seeds [J]. New agriculture, 2017(07):4-6.

[12] Zhang J, Pan S, Zhu J, Chen Z, Hu B, Chen N, Zhang H. Research on calibration method of forward scattering visibility meter based on laser cavity enhancement technology [J]. Journal of light scattering, 2019, 31(02):160-165.

[13] Li J, Liu Y. Frequency domain optimization design of image system [J]. Applications of electronic technology, 2019, 45(07):107-111+116.

International Journal of Computer Applications Technology and Research
Volume 8–Issue 08, 319-322, 2019, ISSN:-2319–8656
DOI:10.7753/IJCATR0808.1005

Genetic Algorithm based Cosmetic Product Forecasting

Khin Aye Mar
Faculty of Computing
University of Computer Studies (Mandalay)
Mandalay, Myanmar

Abstract: The resulting greedy GA favours objects with higher value densities when it builds random chromosomes, in crossover, and in mutation. The greedy heuristics do well, as does the naive GA, but the greedy GA exhibits the best performance. Genetic algorithms initiate the process of evolution on an optimization problem This system is combined greedy idea and genetic algorithm to form the greedy genetic algorithm which incorporates the global exploring ability of the genetic algorithm and the local convergent ability of the greedy algorithm. In this system, population evolution utilizes quantity of sales for cosmetic goods as integer variables. And this system includes fitness function for requirement of profit amount and quantity of products can be calculated by the specific formula. Then, the selection is performed with method of roulette wheel selection. The final result is the forecasting of cosmetic goods for monthly. The greedy genetic algorithm (GGA) always chooses the best goods during the crossover and mutation process according to their fitness values.

Keywords: Genetic algorithm, crossover, mutation, fitness function, initial population

1. INTRODUCTION

Genetic algorithms are a type of optimization algorithm, meaning they are used to find the optimal solution(s) to a given computational problem that maximizes or minimizes a particular function. Greedy Genetic algorithms (GGA) are general- purpose, parallel search techniques for solving complex problems. GGA works by repeatedly modifying a population of artificial structures through the application of genetic operators. A GGA maintains a population of feasible solutions, also known as chromosomes on which the concept of the survival of the fittest among string structures is applied. This system is applied greedy genetic algorithm for forecasting of cosmetic products in the business application [5, 7].

This system represents an optimization approach to a real-world product forecasting problem and will forecast the products by using greedy genetic algorithm. This system is discovered near optimal solutions for business area within an acceptable time. This system also provides a statement for effectively sampling large search spaces and forecast products for the future in business application. The remaining of sections are described theoretical background of the system. Section 3 discusses greedy genetic algorithm for cosmetic product forecasting. Section 4 describes system design. Section 5 explains the implementation results of cosmetic goods forecasting using greedy genetic algorithm in step by step processing. Finally, Section 6 presents conclusion, limitations and future plan of the system.

2. GENETIC ALGORITHM

The simple GA is composed of population of strings, or chromosomes, and three evolutionary operators: selection, crossover, and mutation. The chromosomes may be binary-coded, or they may contain characters from a larger alphabet. The initial population is typically generated randomly, but it may also be supplied by the user.

Genetic Algorithms (GAs) are adaptive heuristic search algorithm premised on the evolutionary ideas of natural selection and genetic. The basic concept of GAs is designed to simulate processes in natural system necessary for evolution, specifically those that follow the principles first laid down by Charles Darwin of survival of the fittest. As such they represent an intelligent exploitation of a random search within a defined search space to solve a problem. [4

2.1 Greedy Genetic Algorithm

The greedy genetic algorithm (GGA) is similar to the classical genetic algorithm (CGA) except for the operation of choosing offsprings in the crossover and mutation. Genetic algorithms (GA's) imitate the process of evolution on an optimization problem. Each feasible solution of a problem is treated as an individual whose fitness is governed by the corresponding objective function value. A GA maintains a population of chromosomes on which the concept of the survival of the fittest (among string structures) is applied.

```
algorithm genetic;
begin
      obtain initial population;
repeat
    select two individuals I1 and I2 in the population;
    apply the crossover operator on I1 and 12 to produce
    a child 13;
   choose two individuals out of I1, I2 and 13;
   occasionally perform immigration;
until the population converges;
end;
```

Figure. 1The Greedy Genetic Algorithm

There is a structured yet randomized information exchange between two individuals *(crossover* operator) to give rise to better individuals. Diversity is also added to the population by

International Journal of Computer Applications Technology and Research
Volume 8–Issue 08, 319-322, 2019, ISSN:-2319–8656
DOI:10.7753/IJCATR0808.1005

randomly changing some genes *(mutation* operator) or bringing in new individuals *(immigration* operator). A GA repeatedly applies these processes until the population converges. The Greedy Genetic Algorithm is illustrated in figure 1 [1, 7].

3. GGA FOR COSMETIC GOODS FORECASTING

This system combines greedy idea into the genetic algorithm. To build string for its initial population, the greedy GA begins by computing the absolute value densities (2) of all the objects. To build each string, the GA considers the objects one at a time. The object to consider next is determined by a tournament with replacement of two objects randomly chosen from those not previously considered.

3.1 Initial Population as Integer

An individual is represented by a set of unsigned integer numbers. Values may be restricted to a finite set. This can be formulated as GAs operate on a number of potential solutions, called a population, consisting of some encoding of the parameter set simultaneously [1]. An example of integer representation of strings is shown in figure 2.

Strings v_1	23 45 55 30 38 58
Strings v_2	44 35 21 56 27 39

Figure.2 Integer representation of Initialization

3.2 Two-Site Crossover

This operator randomly selects two crossover points within a string, and then interchanges the two parent strings between these points to produce two new offsprings. Two site crossover is a variation of the one site crossover, except that two crossover sites are chosen and the bits between the sites are exchanged. [2]. An example of two site crossover is shown in figure 3.

	Before crossover		After crossover
String 1	011|**011**|00	String 1	011|*110*|00
String 2	110|*110*|01	String 2	011|**011**|01

Figure.3 Two site crossover operation

The GGA does not directly accept two offsprings v_1' and v_2' as CGA does. Compute the fitness of $\{v_1, v_2, v_1', v_2'\}$. Then choose two best chromosomes from theses four as the "offsprings" according to their fitness values [7].

3.3 Random Resetting Mutation

In natural evolution, mutation is a random process where one allele of a gene is replaced by another to produce a new genetic structure. In GAs, mutation is randomly applied with low probability, typically in the range 0.001 and 0.01, and modifies elements in the string. An example of random resetting mutation is shown in figure 4.

Original Offspring v	23 45 **21** 56 27 58
Mutated Offspring v'	23 45 **33** 56 27 58

Figure. 4 Random resetting mutation

3.4 Stopping Criterion

The stopping criterion is used in the evaluation process to determine whether or not the current generation and the best solution found so far are close to the global optimum. The standard stopping criteria is used to stop the procedure after the given number of iterations. And, another is used to stop after the 'best' solution has not changed over a specified number of iterations. Another stopping criterion is used when the average fitness of the generation is the same or closes to the fitness of the 'best' solution. In this system, the stopping criterion is used to stop the procedure after a given number of iterations [3].

3.5 Fitness Function

In order to efficiently use the criterion function, it is necessary to define a fitness function which properly assesses the decision rules. The fitness function takes as an input a set of feature or attribute definitions, a set of decision rules. The fitness function or evaluation function plays an important role in a GGA.

The fitness of individuals was evaluated base upon their ability to correctly predict monthly sales data for the product and profit. The fitness of this system means the amount of product for next month that is the best individual. This system defines f (v_i), the fitness of individual i, according to [2,6]

$$f(v_i)= \frac{1}{1+\alpha}$$

where,

$$\alpha = \frac{1}{t}\sum_{j=1}^{N}(x_i - \overline{x}_{ik})^2 + \sum_{i=1}^{N}(x_i NP_i - \overline{x}_{ik} NP_i)\Big| + \wedge$$

NP_i= GP_i - Expenses

GP_i = Sales- Cost of Sales

and where

α = forecast amount of product with profit

$\wedge$ = $10^{-5}\times$(chromosome length), is a penalty term that favors shorter genetic programs over longer ones.

t = the number of months in training set

International Journal of Computer Applications Technology and Research
Volume 8–Issue 08, 319-322, 2019, ISSN:-2319–8656
DOI:10.7753/IJCATR0808.1005

N = chromosome length
x_i = the actual sales of products for each individual v_i
$\hat{x}_{i,k}$ = the forecast of products for each individual v_i
NP_i = net profit for each product
GP_i = gross profit for each product

3.6 Roulette Wheel Selection

The commonly-used reproduction operator is the proportionate reproduction operator where a string is selected for the mating pool with a probability proportional to its fitness. Thus, the ith string in the population is selected with a probability proportional to Fi. Since the population size is usually kept fixed in a simple GA, the sum of the probability of each string being selected for the mating pools must be one. the probability for selecting the ith string is

$$p_i = \frac{\mathcal{F}_i}{\sum_{i=1}^{n} \mathcal{F}_i}$$

where n is the population size. One way to implement this selection scheme is to imagine a roulette-wheel with it's circumference marked for each string proportionate to the string's fitness. The roulette-wheel is spun n times. each time selecting an instance of the string chosen by the roulette-wheel pointer. The average fitness of the population is calculated as

$$F_i = \sum_{i=1}^{n} f_i$$

4. SYSTEM FLOW DIAGRAM

This system uses 56 kinds of cosmetic goods. At the beginning, it retrieves actual sales data for 24 months (two years) as product strings from the database. For example, 5 kinds of cosmetic goods for 4 months as strings are shown in figure 5. In this figure, v1, v2, v3 and v4 are month 1, 2, 3, 4 and the short terms are mean as: S01 = lipstick, S02= Eyes harrow, S03= Body Lotion, S04=Makeup, S05= Toner.

Strings (Monthly)	S01	S02	S03	S04	S05
V1	35	40	45	39	51
V2	44	33	58	42	53
V3	28	54	31	53	48
V4	50	26	29	23	36

Figure. 5 Initial population generation of goods string

Then, the system calculates the fitness value for each goods string based on quantity of sales data, forecast values, profit, time interval and expenses to forecast the goods for the future. The system prompts the user to input number of iteration to be continued to get optimal solution of the forecasted goods.

After that, the system processes probability of the goods string, selecting products by using roulette-wheel selection method, exchanging between goods with two-point crossover operators, mutating the new goods string (offsprings) with random resetting mutation operators, and calculates fitness of the new goods chromosomes. At the stages of crossover and mutation, the system chooses the best chromosomes according to GGA. After completion above processes, the system checks whether it reaches final loop of iteration. If the system reaches final iteration, then it terminates the process and displays the optimal solution of the forecasted amount of goods for the future. The process flow of the system is shown in figure 6.

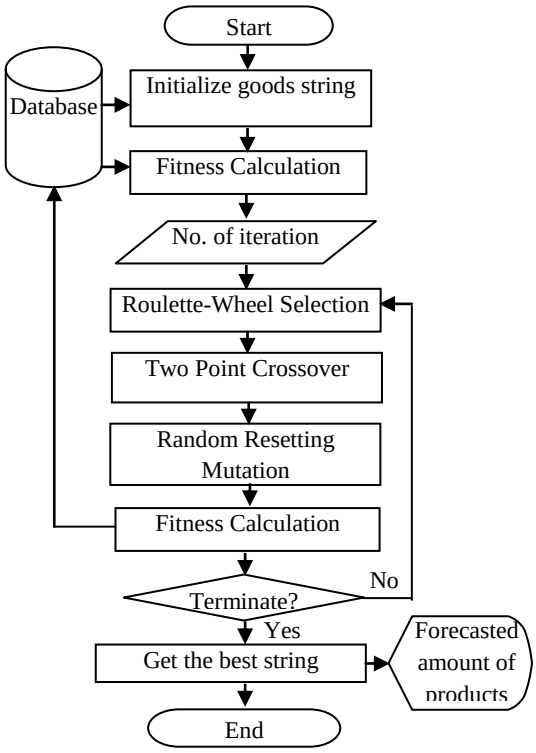

Figure. 6 System flow diagram

5. EXPERIMENTAL RESULT

Initially many individual solutions (actual monthly sales of products) are generated from the database to form an initial population. The control parameters are determined by a GA based on the fitness value calculated from the profit, time interval, actual and forecast sales of goods as shown in figure 7.

In roulette wheel selection, individuals are selected based on the probability that is directly proportional to their fitness value. The crossover is used to goods new solution. After crossover there are two parents and two new solutions. Then compare the fitness of these four solutions and choose the best

International Journal of Computer Applications Technology and Research
Volume 8–Issue 08, 319-322, 2019, ISSN:-2319–8656
DOI:10.7753/IJCATR0808.1005

two solutions as offsprings. In mutation, the fitness of original offspring and mutated offspring are computed and choose the better string as the offspring.

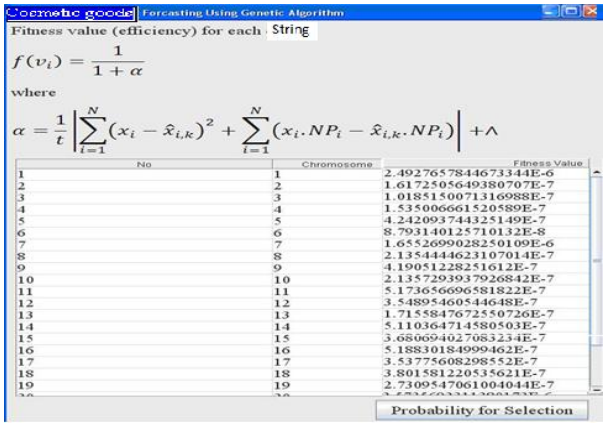

Figure. 7 Fitness calculation for goods

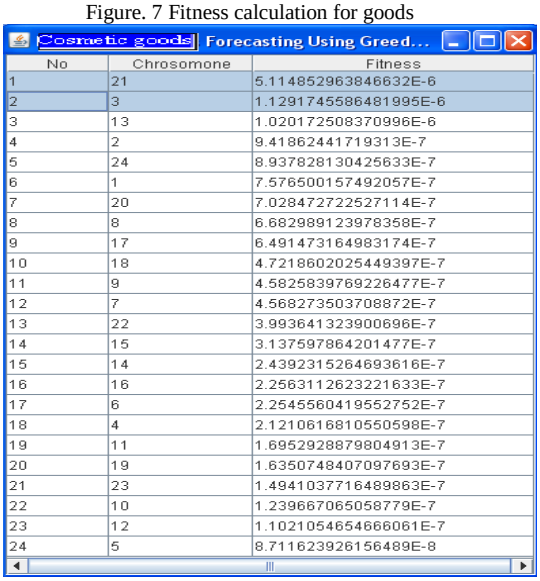

Figure. 8 The fitness values for best forecasted cosmetic goods

For the initial implementations, other control parameters were based on those suggested in popular GA: chromosome length is 56, population size is 24 months, and crossover probability is 0.67 and mutation probability is 0.003.

6. CONCLUSION, LIMITATIONS AND FUTURE PLAN

The power of GAs comes from the fact that the technique is robust, and can deal successfully with a wide range of problem areas, including those which are difficult for other methods to solve. GAs are not guaranteed to find the global optimum solution to a problem, but they are generally good at finding acceptably good solutions to problems acceptably quickly.In this system, integer representation for string are easy to understand and can represent a large number of populations for large search space. By defining meaningful fitness function, the objective of the system can be achieved effectively and quickly. In this system, GGA always chooses the best string during the crossover and mutation process. This may give more satisfy results even the population is small.

In business application, there can have difficulty to forecast the goods manually if there are too large amount of datasets. So, this system can produce the result effectively and quickly by using GGA. Because cosmetic goods in business application are using as data sets in this system, user want to perform in practical that gets result within a short time.

The system can provide the user to forecast the goods for future in business application within acceptable time. By using this system, user can obtain the preferred solution for market such as profit, products and general expenses for future.

This system can extend to forecast large numbers of data sets such as entertainment products and telecommunication products for long-term. This system can only be solved to forecast cosmetic goods for monthly.

References

[1] Bc.Marek Hrusovsky, "Genetic Algorithm Acceleration Using OpenCL" Department of Computer Systems, Brno University of Technology, 2010.

[2] Craenen, B. C. W., Eiben, A. E. and Marchiori, E., How to Handle Constraint with Evolutionary Algorithms. In L. Chambers (Ed.)"The Practical Handbook of Genetic Algorithms"Applications, 2nd Edition, volume 1, Chapman & Hall/CRC, 2001, pp. 341 – 361.

[3] Edwin N., Paul A., Marshall Mc B., Ron L. and Claudelte O., "Modeling and Simulation Optimization Using Evolutionary Computaion", COLSA Corporation, 6726 Odyssey Drive Huntsville, Al 35806, 256-964-5295, 256-964-5355.

[4] Mitchell Melanie, An Introduction to Genetic Algorithms, A Bradford Book The MIT Press Cambridge, Massachusetts, London, England Fifth printing, 1999, First MIT Press paperback edition, 1998

[5] Ravindra k. Ahuja, James B.Orlin, Ashish Tiwari,"A Greedy Genetic Algorithm for the Quadratic Assignent Problem", University of Florida, Gainesville, Massacussetts Institute of Technology, Cambridge, State University of New York, Stony Brook.

[6] Stephen D.Sloan, Raymond W.Saw, James J.Sluss, JR.,Monte P.Tull, and Joseph P.Havlicek, "Genetic Algorithm Forecasting for Telecommunications Products", School of Electrical and Computer Engineering, University of Oklahoma, Norman, Oklahoma.

[7] ZHAO Xinchao, "A Greedy Genetic Algorithm for Unconstrained Global Optimization", Key laboratory of Mathematics, Institute of System Science, AMSS, Chinese Academy of Sciences, Beijing 100080, China.

International Journal of Computer Applications Technology and Research
Volume 8–Issue 08, 323-326, 2019, ISSN:-2319–8656
DOI:10.7753/IJCATR0808.1006

Performance Comparison of Symmetric Key Crypto System

Thet Naing Htwe
Information Technology Department,
Technological University (Kyaukse)
Mandalay, Myanmar

Nilar Htwe
Faculty of Information Science
University of Computer Studies (Mandalay)
Mandalay, Myanmar

Abstract: Security is the most challenging aspects in the internet and network applications. Internet and networks applications are growing very fast, so the importance and the value of the exchanged data over the internet or other media types are increasing. Data confidentiality and authentication are normally provided using cryptographic techniques. Cryptography is either based on symmetric keys or asymmetric keys. This paper provides a fair comparison between three most common symmetric key cryptography algorithms: DES, AES, and RC5. Since main concern here is the performance of algorithms under different settings, the presented comparison takes into consideration the behavior and the performance of the algorithm when different data loads are used. Based on implementation and study, runtime comparison between the symmetric cryptosystems has been made.

Keywords: Symmetric Key System, AES, DES, RC5,

1. INTRODUCTION

Symmetric Encryption algorithms play a primary role in information security. So this paper has surveyed the most common algorithms and standards available for the encryption of information in the digital form. An encryption algorithm would be useless if it is secure but takes long time in execution. The field of cryptography is becoming very important in today's times as information security is of absolute importance. Contemporarily more and more sensitive data is being stored on computers and transmitted over the Internet. We need to ensure security and safety of information.

Cryptography is used to protect data while it is being communicated between two points. Cryptography is either based on symmetric keys or asymmetric keys [1]. This paper analyzes and studies between the most popular symmetric cryptographic algorithms such as data encryption standard, advanced encryption standard, and RC5. Based on analyze and by doing experiment, runtime comparison between the symmetric cryptosystems have been made.

This paper is organized with five sections. The first section is introduction of the system. Section 2 explains theory of Cryptography. Section 3 explains symmetric algorithms used in this paper such as AES, DES and RC4. Section 4 describes the implementation of the system. Experimental result is explained in section 4 and the next section is conclusion of the system.

2. DOCUMENTS OF CRYPTOGRAPHY

Cryptography provides a number of security goals to avoid a security issue. Due to security advantages of cryptography it is widely used today. Two type of Cryptography: Symmetric and Asymmetric. This paper is concerned with Symmetric cryptography [5, 6].

2.1 Symmetric Algorithms

The Symmetric algorithms use the same key for encryption and decryption while asymmetric algorithms use a different key for encryption and decryption, and the decryption key cannot be derived from the encryption key. Symmetric algorithms can be divided into stream ciphers and block ciphers. Stream ciphers can encrypt a single bit of plaintext at a time, whereas block ciphers take a number of bits (typically 64 bits in modern ciphers), and encrypt them as a single unit. There are many cryptographic algorithms. This thesis analyzes and studies three of the most common symmetric algorithms DES, AES and RC5. [5]

The field of cryptography include the following items:

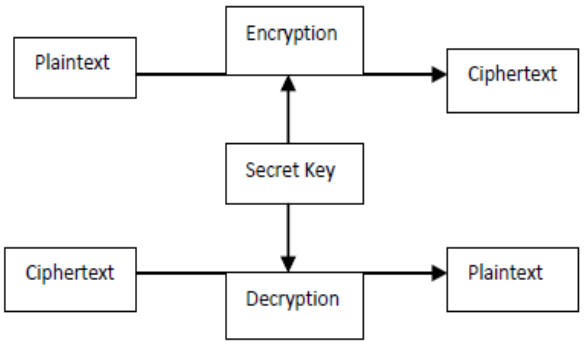

Figure 1 Symmetric Key Cryptography Process

2.1.1 Plain Text

The original message that someone wishes to another is defined as Plain Text. In cryptography the real message that has to be sent to the other end is given a special name as Plain Text. Suppose Alice wishes to send the message, *"We shall meet behind the monument in the garden."* to Bob. Here *"We shall meet behind the monument in the garden."* is the plain text.

International Journal of Computer Applications Technology and Research
Volume 8–Issue 08, 323-326, 2019, ISSN:-2319–8656
DOI:10.7753/IJCATR0808.1006

2.1.2 Cipher Text

The message that cannot be understood by anyone or meaningless message is what we call as Cipher Text. In Cryptography the original message is transformed into non readable message before the transmission of actual message. For example, *"Jr funyy zrrg oruvaq gur zbahzrag va gur tneqra."* is a Cipher Text produced for *"We shall meet behind the monument in the garden."* after applying the Caesar's Cipher with key = 13.

2.1.3 Encryption

A process of converting Plain Text into Cipher Text is called Encryption. Cryptographers use various encryption methods to send confidential messages via an insecure channel. The process of encryption requires two things - an encryption algorithm and a key. An encryption algorithm means the method that has been used in encrypt the data. Encryption happens at the sender's side.

2.1.4 Decryption

The reverse process of encryption is called Decryption. It is the process of converting Cipher Text into Plain Text. Cryptographers use the decryption algorithms at the receiver side to obtain the original message from non readable message i.e. Cipher Text. The process of decryption requires two things - a Decryption algorithm and a key. A Decryption algorithm means the method that has been used in Decryption. Generally the encryption and decryption algorithm are identical but reverse.

2.1.5 Key

A Key is a string of alpha numeric characters, which is used to encrypt & decrypt the message. The Key is used at the time of encryption that works on the Plain Text and at the time of decryption works on the Cipher Text. The selection of key in Cryptography is vital as the security of encryption algorithm depends directly on it. For example, if Alice uses Hill Cipher & a key [11 10 20 09] to encrypt the Plain Text *"Gold is buried under the bush of Red Roses!"* then Cipher Text produced will be *"ymvnikdshwwdmxvsnrnudsihwntmvfwaqi"*.

2.1.6 Encoder

An encoder is the person that wants to send the message & uses encryption to make the message secure.

2.1.7 Decoder

A decoder is the person who decrypts the message. This may be the intended recipient of the message or may be an intruder, trying to get access to the secret message.

3. BACKGROUND STUDY

In this paper symmetric encryption algorithm is used for file transfer system. The security of this symmetric cryptosystem, should not rely on the confidentiality of the algorithm, it depends on the secret of keys [5, 6].

3.1. Data encryption standard (DES)

Data Encryption Standard (DES) DES (Data Encryption Standard) algorithm purpose is to provide a standard method for protecting sensitive commercial and unclassified data. In this same key used for encryption and decryption process [3]. DES algorithm consists of the following steps

For Encryption

1. DES accepts an input of 64-bit long plaintext and 56-bitkey (8 bits of parity) and produce output of 64 bit block.
2. The plaintext block has to shift the bits around.
3. The 8 parity bits are removed from the key by subjecting the key to its Key Permutation.
4. The plaintext and key will processed by following
   i. The key is split into two 28 halves
   ii. Each half of the key is shifted (rotated) by one or two bits, depending on the round.
   iii. The halves are recombined and subject to a compression permutation to reduce the key from 56 bits to 48 bits. This compressed keys used to encrypt this round's plaintext block.
   iv. The rotated key halves from step 2 are used in next round.
   v. The data block is split into two 32-bit halves.
   vi. One half is subject to an expansion permutation to increase its size to 48 bits.
   vii. Output of step 6 is exclusive-OR'ed with the 48-itcompressed key from step 3.
   viii. Output of step 7 is fed into an S-box, which substitutes key bits and reduces the 48-bit block back down to 32-bits.
   ix. Output of step 8 is subject to a P-box to permute the bits.
   x. The output from the P-box is exclusive-OR'ed with other half of the data block. k. The two data halves are swapped and become the next round's input.

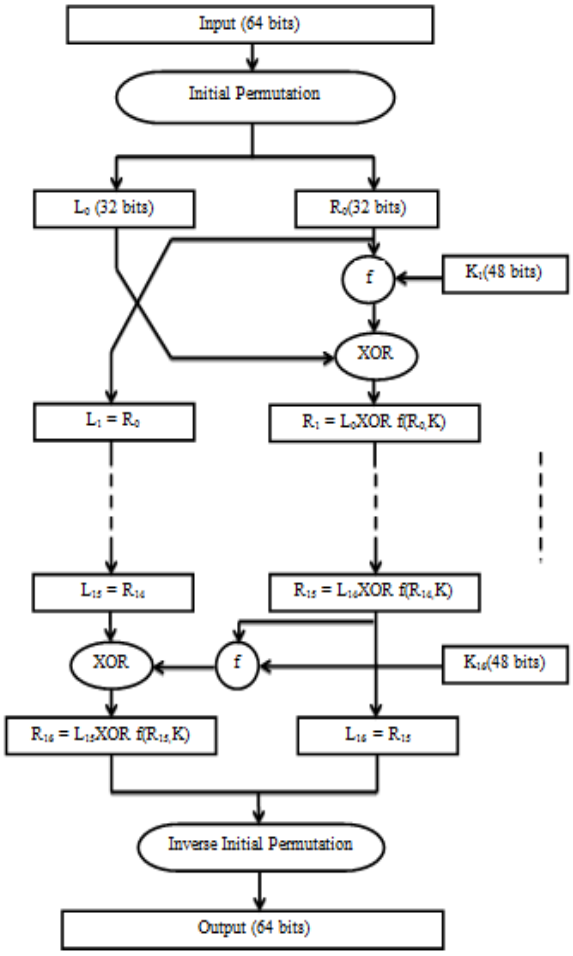

Figure 2 Diagram of DES Algorithm

International Journal of Computer Applications Technology and Research
Volume 8–Issue 08, 323-326, 2019, ISSN:-2319–8656
DOI:10.7753/IJCATR0808.1006

3.2. Advanced Encryption Standard (AES)

AES algorithm uses a round function that is compared of four different byte-oriented transformation such as Sub byte, Shift row, Mix column ,Add round key. Number of rounds to be used depend on the length of key e.g. 10 round for 128 bit key, 12 rounds for 192-bit key and 14 rounds for 256 bit keys.

The algorithm begins with an **Add round key** stage followed by 9 rounds of four stages and a tenth round of three stages. This applies for both encryption and decryption with the exception that each stage of a round the decryption algorithm is the inverse of it's counterpart in the encryption algorithm [4]. The four stages are as follows:

1. Substitute bytes
2. Shift rows
3. Mix Columns
4. Add Round Key

The tenth round simply leaves out the **Mix Columns** stage. The first nine rounds of the decryption algorithm consist of the following:

1. Inverse Shift rows
2. Inverse Substitute bytes
3. Inverse Add Round Key
4. Inverse Mix Columns

Again, the tenth round simply leaves out the **Inverse Mix** Columns stage. Each of these stages will now be considered in more detail.

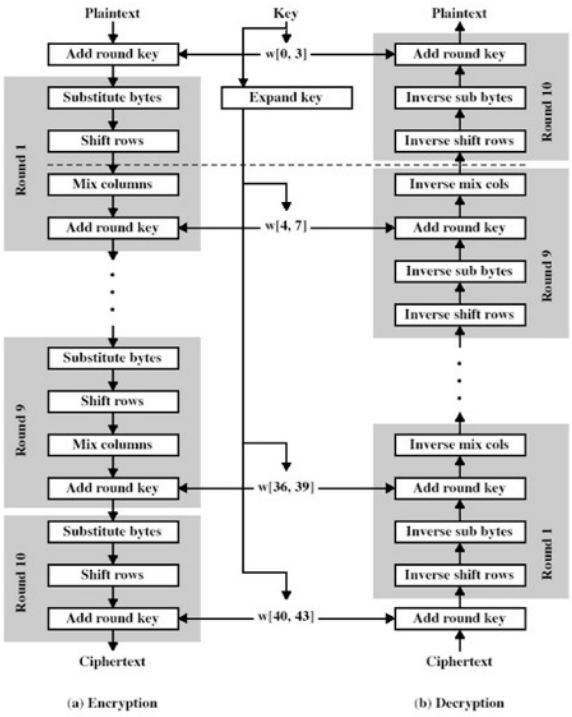

Figure 3. AES encryption and decryption

Figure 3 shows the overall structure of AES. The input to the encryption and decryption algorithms is a single 128-bit block. In FIPS PUB 197, this block is depicted as a square matrix of bytes. This block is copied into the State array, which is modified at each stage of encryption or decryption. After the final stage, State is copied to an output matrix. These operations are depicted in Figure 3a. Similarly, the 128-bit key is depicted as a square matrix of bytes. This key is then expanded into an array of key schedule words; each word is four bytes and the total key schedule is 44 words for the 128-bit key Figure 3b. Note that the ordering of bytes within a matrix is by column. So, for example, the first four bytes of a 128-bit plaintext input to the encryption cipher occupy the first column of the in matrix, the second four bytes occupy the second column, and so on.

3.3. RC5 symmetric algorithm

The RC5 encryption algorithm is a block cipher that converts plain text data blocks of 16, 32, and 64 bits into cipher text blocks of the same length. It uses a key of selectable length b (0, 1, 2, ..., 255) byte. The algorithm is organized as a set of iterations called rounds r that takes values in the range (0, 1, 2, ..., 255) as illustrated in figure 4.

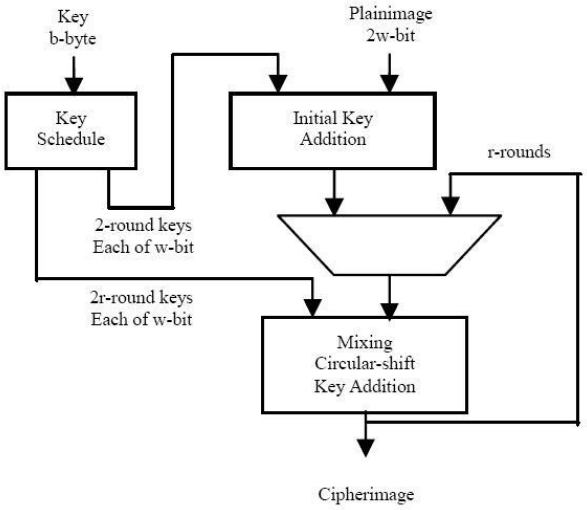

Figure 4 RC5 Encryption Algorithm

3.3.1 Operation of RC5

The operations used in RC5 are defined as followings.

1. A+B integer addition modulo 2w
2. A-B integer subtraction modulo 2w
3. A⊕B bitwise exclusive-or of w-bit words
4. A<<<B rotation of the w-bit word A to the left by the amount given by the least significant lg w bits of B
5. A>>>B rotation of the w-bit word A to the right by the amount given by the least significant lg w bits of B

There are three routines in RC5: key expansion, encryption, and decryption [2, 5]. We discus each of them in next sections, Key-Expansion algorithm is used to generate the round sub keys that will be use in both encryption and decryption algorithms. RC5 has different algorithms for encryption and decryption, in encryption it uses integer addition modulo 2w but in decryption it uses integer subtraction modulo 2w. RC5 is a symmetric key encryption

4. IMPLEMENTATION OF THE SYSTEM

This paper describes the comparison of encryption time and decryption time of three popular symmetric key algorithms. In processing of three algorithms, it compares encryption and decryption time of various file sizes using DES, AES, and RC5 symmetric algorithms and then shows comparison results in table and in graph.

International Journal of Computer Applications Technology and Research
Volume 8–Issue 08, 323-326, 2019, ISSN:-2319–8656
DOI:10.7753/IJCATR0808.1006

Method/File Size (KB)	150	192	306	852	1120
DES	2.9	3.1	3.3	4.1	5.4
AES	1.6	1.7	1.8	2.1	2.2
RC5	3.0	4.8	5.9	6.7	9.0

4.1 Experimental result

The experimental results of encryption and decryption time on various text files using DES, AES, and RC5 algorithms are shown in Table 1, Table 2 and Figure 5 and 6. Table 1 shows the results of comparing encryption time (s) on each various file sizes (KB) using three methods. Table 2 shows decryption time (s) for each various file size (KB). Figure 5 and Figure 6 show results by charts.

Table 1. Comparison of Encryption Time (s)

Method/ File Size (KB)	150	192	306	852	1120
DES	1.1	1.2	1.3	1.4	1.5
AES	1	1.4	1.6	1.8	2.1
RC5	3.1	3.7	4.1	4.7	5.1

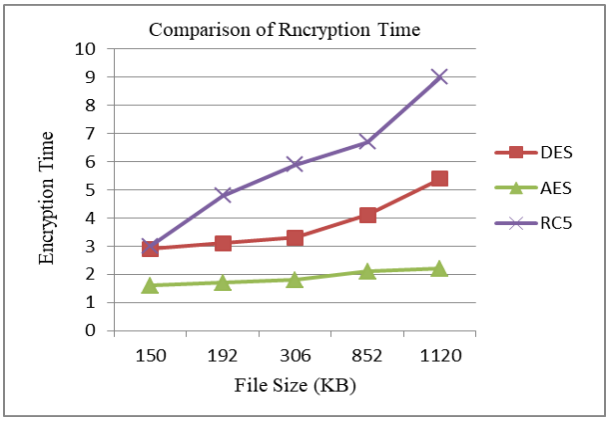

Figure 5. Comparison of Encryption Time

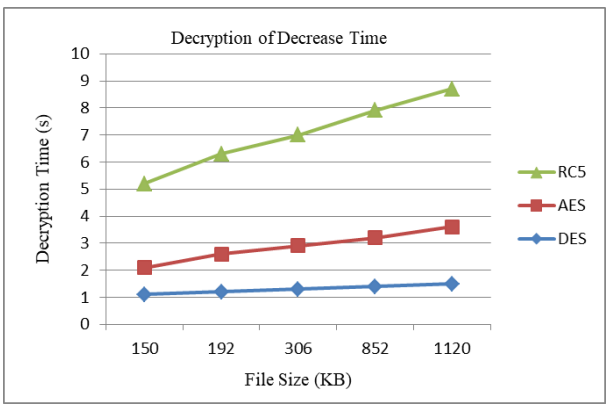

Figure. 6 Comparison of Decryption Time

5. CONCLUSION

This paper has investigated the comparison among the most popular symmetric algorithms. Among several algorithms, this paper describes the comparison of encryption and decryption time of DES, AES, and RC5 methods. After making several testing and comparing three techniques, encryption time is distinctly different but decryption time is not very different.

Based on the text files used and the experimental result it was concluded that AES algorithm consumes least encryption and RC5 consume longest encryption time. We also observed that Decryption of AES algorithm is better than other algorithms. From the simulation result, we evaluated that AES algorithm is much better than DES and RC5 algorithm.

It can be used to learn cryptography and popular symmetric key algorithms, to learn comparing encryption and decryption time of these algorithms. It can be used for only text files format. So, it can be extended for audio file and image file formats and also compare for security point of view of three symmetric algorithms. the information has to be secured though transmit it, Sensitive information like ATM cards, banking dealings and public security numbers require to be secured. Different encryption techniques are used to protect the confidential data from unauthorized use. Encryption is a very general method for promoting the information security. The development of encryption is moving towards a prospect of endless possibilities.

REFERENCES

[1] Ritu Tripathi, Sanjay Agrawal, Comparative Study of Symmetric and Asymmetric Cryptography Techniques, International Journal of Advance Foundation and Research in Computer (IJAFRC) Volume 1, Issue 6, June 2014. ISSN 2348 – 4853

[2] Dr. Prerna Mahajan & Abhishek Sachdeva, A Study of Encryption Algorithms AES, DES and RSA for Security, Global Journal of Computer Science and Technology Network, Web & Security, Volume 13 Issue 15 Version 1.0 Year 2013 Type: Double Blind Peer Reviewed International Research Journal Publisher: Global Journals Inc. (USA), Online ISSN: 0975-4172 & Print ISSN: 0975-4350

[3] Abdel-Karim Al Tamimi, “Performance Analysis of Data Encryption Algorithms”.

[4] Andreas Sterbenz, Peter Lipp, “Performance of the AES Candidate Algorithms in Java”.

[5] William Stallings, *Cryptography and Network Security Principles and Practicle*, Fourth Edition

[6] *http://www.abo.fi/~ipetre/crypto/*

International Journal of Computer Applications Technology and Research
Volume 8–Issue 08, 327-330, 2019, ISSN:-2319–8656
DOI:10.7753/IJCATR0808.1007

Comparative Study of Dynamic Programming and Greedy Method

San Lin Aung
Information Technology, Supporting and Maintenance Department
University of Computer Studies (Mandalay)
Myanmar

Abstract: This paper discusses relationships between two approaches to optimal solution to problems: Greedy algorithm and dynamic programming. Greedy algorithm has a local choice of the sub-problems whereas Dynamic programming would solve the all sub-problems and then select one that would lead to an optimal solution. Greedy algorithm takes decision in one time whereas Dynamic programming takes decision at every stage. This paper discuss about Dynamic Programming and Greedy Algorithm to solve the Knapsack Problem where one has to maximize the benefit of items in a knapsack without extending its capacity. The paper discusses the comparison of each algorithm in terms of time different Item values. The comparison result of two algorithms are described with the best local result produced by the algorithm against the real exact optimal result.

Keywords: Greedy Algorithm, Dynamic Programming, 0/1 Knapsack, Algorithm

1. INTRODUCTION

The Knapsack problem is a combinatorial optimization problem where one has to maximize the benefit of objects in a knapsack without exceeding its capacity. The objective of the paper is to present a comparative study of the dynamic programming, and greedy algorithms. The 0-1 Knapsack Problem is vastly studied in importance of the real world applications. The KP is a: given an arrangement of items, each with weight and a value, decide the number of each item to include in a capacity so that the total weight is little than a given capacity and the total value must as large as possible.

Greedy strategy is to point out the initial state of the problem, through each of the greedy choice and get the optimal value of a problem solving method [8]. Dynamic programming is an optimization approach that transforms a complex problem into a sequence of simpler problems; its essential characteristic is the multistage nature of the optimization procedure. More so than the optimization techniques described previously, dynamic programming provides a general framework for analyzing many problem types. Within this framework a variety of optimization techniques can be employed to solve particular aspects of a more general formulation [2].

The paper is organized as follows: section 2 describes The Knapsack Problem (KP). Section 3 expresses Dynamic Programming and Greedy algorithm. This section also includes example of dynamic algorithm and the basic idea of the greedy algorithm. Section 4 presents Experimental Results and Section 5 illustrates the Conclusion.

2. THE KNAPSACK PROBLEM (KP)

The Knapsack Problem is an example of a combinatorial optimization problem, which seeks for a best solution from among many other solutions. Given a set of items, each with a mass and a value, determine the number of each item to include in a collection so that the total weight is less than or equal to a given limit and the total value is as large as possible. We have n of items. Each of them has a value Vi and a weight Wi.

The 0-1 Knapsack Problem is vastly studied in importance of the real world applications that build depend it discovering the minimum inefficient approach to cut crude materials seating challenge of speculations and portfolios seating challenge of benefits for resource supported securitization, A few years ago the generalization of knapsack problem has been studied and many algorithms have been suggested [1]. Advancement Approach for settling the multi-objective0-1 Knapsack Problem is one of them, and there is numerous genuine worked papers established in the writing around 0-1 Knapsack Problem and about the algorithms for solving them.

The 0-1 KP is extremely well known and it shows up in the real life worlds with distinctive application. The most extreme weight that we can convey the knapsack is C. The 0 – 1 KP is an uncommon case of the original KP problem in which each item can't be Sub separated to fill a holder in which that input part fits. The 0 – 1 KP confines the quantity of each kind of item xj to 0 or 1. Mathematically the 0 – 1 KP can be formulated as: [1, 3, 4]

$$\text{Maximize} \sum_{i=1}^{n} \mathbf{Pi\ Xi} \text{ Subject to } \sum_{i=1}^{n} \mathbf{Wi\ Xi} \leq C$$

International Journal of Computer Applications Technology and Research
Volume 8–Issue 08, 327-330, 2019, ISSN:-2319–8656
DOI:10.7753/IJCATR0808.1007

3. DYNAMIC PROGRAMMING AND GREEDY ALGORITHM

Dynamic algorithm is an algorithm design method, which can be used, when the problem breaks down into simpler sub problems; it solves problems that display the properties of overlapping sub problems. In general, to solve a problem, it's solved each sub problems individually, then join all of the sub solutions to get an optimal solution [2, 5].

The dynamic algorithm solve each sub problem individually, once the solution to a given sub problem has been computed, it will be stored in the memory, since the next time the same solution is needed, it's simply looked up. Distinctly, a Dynamic algorithm guarantees an optimal solution.

Dynamic Programming is a technique for solving problems whose solutions satisfy recurrence relations with overlapping subproblems. Dynamic Programming solves each of the smaller subproblems only once and records the results in a table rather than solving overlapping subproblems over and over again. To design a dynamic programming algorithm for the 0/1 Knapsack problem, we first need to derive a recurrence relation that expresses a solution to an instance of the knapsack problem in terms of solutions to its smaller instances. Consider an instance of the problem defined by the first i items, 1<= i<= N, with:

weights w1, ... , wi,
values v1, ... , vi,
and knapsack capacity j, 1<= j<= Capacity.

3.1 Algorithm Dynamic Programming

ALGORITHM Dynamic Programming
(Weights [1 ... N], Values [1 ... N], Table [0 ... N, 0 ... Capacity])
//Input: Array Weights contains the weights of all items
Array Values contains the values of all items
Array Table is initialized with 0s; it is used to store the results from the dynamic programming algorithm.
// Output: The last value of array Table (Table [N, Capacity])
contains the optimal solution of the problem for the given Capacity
for i = 0 to N do
for j = 0 to Capacity
if j < Weights[i] then Table[i, j] ←Table[i-1, j]
else Table[i, j] ← maximum { Table[i-1, j] AND Values[i] + Table[i-1, j – Weights[i]]
return Table [N, Capacity]

3.2 An Elementary Example

In order to introduce the dynamic-programming approach to solving multistage problems, in this section we analyze a simple example. Figure 1 represents a street map connecting homes and downtown parking lots for a group of commuters in a model city. The arcs correspond to streets and the nodes correspond to intersections. The network has been designed in a diamond pattern so that every commuter must traverse five streets in driving from home to downtown. The design characteristics and traffic pattern are such that the total time spent by any commuter between intersections is independent of the route taken. However, substantial delays, are experienced by the commuters in the intersections. The lengths of these delays in minutes, are indicated by the numbers within the nodes. We would like to minimize the total delay any commuter can incur in the intersections while driving from his home to downtown. [6, 7]

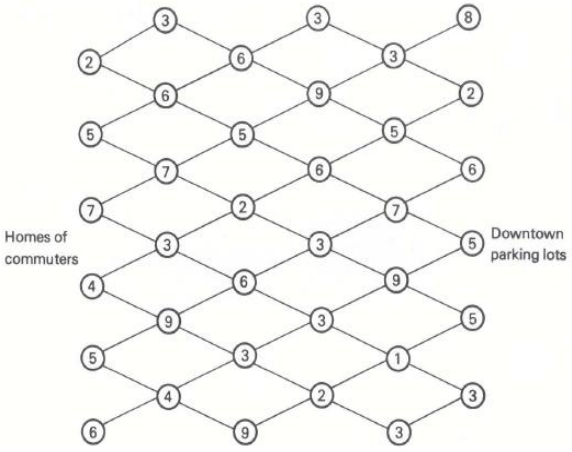

Figure1. Street map with intersection delays.

Figure 1 provides a compact tabular representation for the problem that is convenient for discussing its solution by dynamic programming. In this figure, boxes correspond to intersections in the network. In going from home to downtown, any commuter must move from left to right through this diagram, moving at each stage only to an adjacent box in the next column to the right. We will refer to the ‘‘stages to go," meaning the number of intersections left to traverse, not counting the intersection that the commuter is currently in.

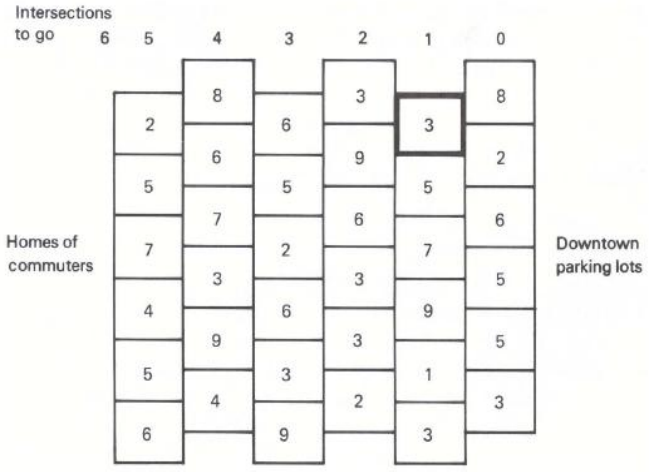

Figure 2. Compact representation of the network.

International Journal of Computer Applications Technology and Research
Volume 8–Issue 08, 327-330, 2019, ISSN:-2319–8656
DOI:10.7753/IJCATR0808.1007

The most naive approach to solving the problem would be to enumerate all 150 paths through the diagram, selecting the path that gives the smallest delay. Dynamic programming reduces the number of computations by moving systematically from one side to the other, building the best solution as it goes. Suppose that we move backward through the diagram from right to left. If we are in any intersection (box) with no further intersections to go, we have no decision to make and simply incur the delay corresponding to that intersection. The last column in Figure 2 summarizes the delays with no (zero) intersections to go [6, 7].

3.3 Greedy algorithm

A greedy algorithm is a straight forward design technique, which can be used in much kind of problems. Mainly, a greedy algorithm is used to make a greedy decision, which leads to a feasible solution that is maybe an optimal solution. Clearly, a greedy algorithm can be applied on problems those have 'N' number of inputs and we have to choose a subset of these input values those satisfy some preconditions.

Where, the next input will be chosen if it is the most input that satisfies the preconditions with minimizes or maximizes the value needed in the preconditions. A greedy algorithm is a straight forward design technique, which can be used in much kind of problems. Mainly, a greedy algorithm is used to make a greedy decision, which leads to a feasible solution that is maybe an optimal solution [4, 8].

3.4 The basic idea of the greedy algorithm

Greedy algorithm is a step by step, according to a certain optimization measure; each step should be able to ensure that the local optimal solution can be obtained. If the next data and partial optimal solution is no longer feasible solution, then the data cannot be added to the partial optimal solution until all the data are enumerated or cannot be added so far.

The hierarchical processing method of the optimal solution which can be obtained by some kind of measure is called the greedy strategy. If you want to use the greedy strategy to solve the problem, it is necessary to solve the following two problems: [4, 8]

(1) Whether the problem can be solved by greedy strategy;

(2) How to determine the greedy choice strategy, to get the best or better solution.

3.5 Algorithm Greedy Algorithm

ALGORITHM GreedyAlgorithm (Weights [1 ... N], Values [1 ... N])
// Input: Array Weights contains the weights of all items
Array Values contains the values of all items
// Output: Array Solution which indicates the items are included in the knapsack ('1') or not ('0')
Integer CumWeight
Compute the value-to-weight ratios ri = vi / wi, i = 1, ..., N, for the items given Sort the items in non-increasing order of the value-to-weight ratios for all items do
if the current item on the list fits into the knapsack
then place it in the knapsack
else proceed to the next one

4. COMPARISON RESULTS

KP is a well-known optimization problem, which has restriction of the value either 0 (leave it) or 1 (take it), for a given collection of items, where each has a weight and a value, that to determine the items to be included in a sets, then the total cost is less or equal to a given capacity and the total profit is as max as possible.

For testing, different file sizes are generated integers representing the weight and value of each item. We are test all of them using different array size but with the same Capacity size on 50, 100, 200, and 500. Sample result of testing for capacity = 50 is as shown in table 1 and figure 3.

Table 1 Comparison for Capacity = 50

Number of Items	Total Value GA	Total Value DP
100	1360	1385
200	3100	3320
300	5400	5600
400	8250	8535
500	13500	13700

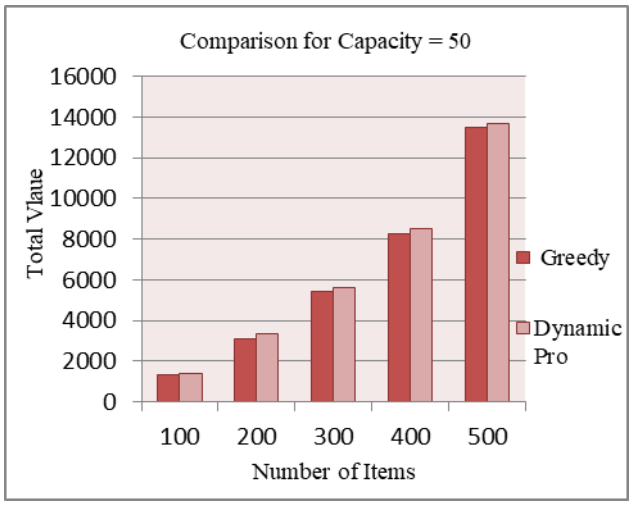

Figure 3 Comparison of Dynamic Programming and Greedy Algorithm

5. CONCLUSION

We can conclude that dynamic programming algorithms outperform and the greedy and genetic algorithm in term of the total value it generated. Greedy algorithm lacks with parallelism property whereas Dynamic Algorithm are exposed to parallelism. Both Greedy and Dynamic programming algorithm try to find out the optimal solution.

In both algorithm an optimal solution to the problem contains within it optimal solutions to sub-problems. Greedy method work efficiently for some problems like Minimum Spanning tree while it is not best suited for some problem like Travelling Sales man ,0/1 Knapsack. Dynamic method always generates optimal solution but they are less efficient than Greedy algorithm. As Greedy algorithm are generally fast.

Hence, paper presents a comparative study of the Greedy and dynamic methods. It also gives complexity of each algorithm with respect to time and space requirements. A feasible solution that does this is called an optimal solution. In order to solve a given problem, each problem has N inputs and requires finding a feasible solution that either maximizes or minimizes a given objective function that satisfies some constraints.

REFERENCES

[1] AuGallo, G.; Hammer, P. L.; Simeone, B. (1980). "Quadratic knapsack problems". Mathematical Programming Studies 12: 132–149.
[2] Kleywegt, D.Papastavrou, “The Dynamic and Stochastic knapsack Problem,” Opns. Res, pp. 17–35, 1998.
[3] M. Hristakeva, D. Shrestha, “Solving the 0-1 Knapsack Problem with Genetic Algorithms,” IEEE Transl. Beijing, Science & Math Undergraduate Research Symposium, Indianola, Iowa, Simpson College June 2004.
[4] M.Lagoudakis, “The 0–1 knapsack problem—an introductory survey citeseer.nj.nec.com/151553.html, 1996.
[5] S. Martello, D. Pisinger, P. Toth “Dynamic Programming and Strong Bounds for the 0-1 Knapsack Problem,” Management Science, vol. 45, pp. 414–424, 1999
[6] http://en.wikipedia.org/wiki/Dynamic_programming
[7] http://www.geeksforgeeks.org/dynamic-programmingset-23-bellman-ford-algorithm/
[8] http://en.wikipedia.org/wiki/Greedy_algorithm

International Journal of Computer Applications Technology and Research
Volume 8–Issue 08, 331-339, 2019, ISSN:-2319–8656

Human Ability Improvement with Wireless Sensors in Human Computer Interaction

Alao, O.D
Department of Computer Science
School of Computing and Engineering Sciences,
Babcock University
Ogun State. Nigeria.

Joshua J.V
Department of Computer Science
School of Computing and Engineering Sciences,
Babcock University
Ogun State. Nigeria.

Somefun A.A
Department of Computer Science
School of Computing and Engineering Sciences,
Babcock University
Ogun State. Nigeria.

Abstract: Wireless sensors are nowadays engaged in almost every human endeavour and has made live more convenient and conducive. Human Computer interaction (HCI), which is about communication between human user and computer system or devices is a field of computer science that is gaining a lot of recognition in the improvement of human abilities. The communication between a person or user and the computer may involve certain device, medium or channel that has to be configured or programmed in a way that will facilitate an efficient interaction.
Wireless sensors in HCI enhances and improves the way of life and the interaction in a wide variety of domains Therefore, it is important to know the specifications of these sensors and how they are being used in order to create human computer interfaces, which tackle complex tasks.
This paper comprehensively carried out an overview of wireless sensors and HCI, security requirements and challenges of wireless sensors and how wireless sensors interrelate with HCI to improve human abilities in their daily activities. Finally, a brief discussion on the future of sensors in HCI is presented.

Keywords; Sensors, Human Ability, Human-Computer Interaction, Modality and Activity Sensing

1. INTRODUCTION

With sensors employed in almost every aspect of lives, it has improved the well-being of people. Sensor is a device that detects, senses physical stimulus such as heat, light, sound, motion, etc and then respond or react to it in a particular way and transmits a resulting impulse. The application of wireless sensors has greatly improved and imparted utilization of many system units for example, television with remote control or automatic door system. Also, the integration of sensors and networking technologies has enabled the development of new applications in a wide variety of domains such as, smart homes, e-health, and intelligent transport systems. (Paravati and Gatteschi, 2015)

Automatic recognition of physical activities commonly referred to as human activity recognition (HAR) has emerged as a key research area in human-computer interaction (HCI) and mobile and ubiquitous computing. One goal of activity recognition is to provide information on a user's behaviour that allows computing systems to proactively assist users with their tasks. Human activity recognition requires running classification algorithms, originating from statistical machine learning techniques. Mostly, supervised or semi-supervised learning techniques are utilized and such techniques rely on labelled data, i.e., associated with a specific class or activity. In most of the cases, the user is required to label the activities and this, in turn, increases the burden on the user. (Sunny, George and Kizhakkethottam, 2015)

The presence of sensors in wireless technology with components like microprocessor, microcontroller makes technology omnipresent and increasingly embedded into the environment. This brings intelligence into various applications like intelligent factories, smart homes, intelligent building, smart environment etc. Wireless sensor has broken the bond where user can only interact with one stationary device and make rooms for concept where user interacts with the environment. This is made possible through interface technologies like speech interaction, gesture recognition, eye-tracking and wearable devices.

The future of human computer interaction systems lies in how intelligently these systems with the use of wireless sensors can take into account the user's context. Furthermore, research on recognizing the daily activities of people has progressed steadily, but little focus has been devoted to recognizing joint activities as well as movements in a specific activity. For many applications such as rehabilitation, sports medicine, geriatric care, and health/fitness, monitoring the importance of combined recognition of activity and movements can drive health care outcome (Varkey, Pompili, & Walls, 2012)

This paper discusses the role of wireless sensors in facilitating seamless communications between human and computer, a comprehensive review of some application areas of the

wireless sensors technology in HCI, associated challenge of wireless sensorss and how they interrelate with HCI to improve human abilities in their daily activities. The paper concludes with a brief discussion on the future of sensors in HCI.

2. Overview of Sensors

A sensor is an electronic device used to detect or measure a physical quantity and convert it into an electronic signal. In other words, sensors are devices that translate aspects of physical reality into a representations understandable and can be processed by computers. Fritzsche (2015) defined a sensor is an object performing a sensing task, gathering information about an object or a process, including the occurrence of events. A sensor technically acts as a transducer which transforms physical signals to electrical energy. Sensors link the physical with the digital world by capturing and revealing real-world phenomena and converting these into a form that can be processed, stored, and acted upon (Dargie & Poellabauer, 2010). Sensors have been known to drive computer automation and vision over the years (Hua, et al., 2017). Sensors are the pedestal components on which object tracking is based; and object tracking, in turn, has been extensively studied in computer vision due to its applications in surveillance, human-computer interaction, video indexing, and traffic monitoring, to name a few.
Sensors continue to rapidly evolve, becoming increasingly smaller, cheaper, more accurate, more reliable, efficient, responsive and with increasing communication capability. These key factors as well as the availability of new technologies are contributing to the growth of the market of consumer electronics sensors, thus reducing their costs. This scenario has fostered the embedding of sensors in the everyday objects of our lives (Paravati and Gatteschi 2015).

2.1 Types of Sensors:

Sensors can be classified based on power or energy supply requirement of the sensors as passive and active sensor.

2.1.1 Passive sensor

Passive sensors require an external power source to operate, which is called an excitation signal. The signal is modulated by the sensor to produce an output signal. For example, a thermistor does not generate any electrical signal, but by passing an electric current through it, its resistance can be measured by detecting variations in the current and/or voltage across the thermistor (Fraden, 2016).

2.1.2 Active sensor

Active sensors generate electric signals in response to an external stimulus without the need of an additional energy source. Examples of active sensors are photodiode, piezoelectric sensor and a thermocouple (Kalantar-zadeh, 2013).

Another way of classifying sensors is with regards to the physical property they measure. The most common categories include Mechanical, Thermal, Electrical, Magnetic, Radiation, Chemical and Bio-chemical**.** Sensors can alternatively be classified according to the following criteria primary input quantity (for measurement), transduction principles (using physical and chemical effects), material and technology, property and application

2.2 Functionality of Sensors

According to Spencer et al (2014), for sensor to function and communicate, it has to be integrated with other component. A traditional integrated sensor can be divided into three parts as shown in figure 1
(i) The sensing element (e.g photo diode, light dependent resistor, piezo-electric material)
(ii) Signal conditioning and processing element (e.g for amplifications, linearization, compensation, and filtering)
(iii) A sensor interface (e.g. the wires, plugs and sockets to communicate with other electronic components)

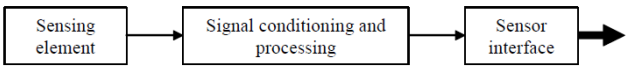

Figure 1: Traditional Integrated Sensors

Source: (Spencer, Manuel, & Narito, 2014)

Table 1: Examples of Sensors with Their Measured Property and Application type

Sensor	**Measured Property**	**Application Type**
Accelerometer	Acceleration	Activity sensing, Context sensing, Environment sensing, Physiological state sensing
Air pollutants sensors	Amount of toxic particles in the atmosphere	Context sensing, Environment sensing
Barometer	Pressure	Activity sensing, Context sensing, Physiological state sensing
Bluetooth	Radio signals	Activity sensing, Context sensing
Camera	Visual light	Activity sensing, Context sensing,

		Environment sensing, Physiological state sensing
Compass	Earth magnetic field	Activity sensing
Electro cardiogram (ECG or EKG)	Heartbeat	Activity sensing
Electromyography sensor	Electrical activity produced by skeletal muscles	Activity sensing
Gyroscope	Measures orientation	Activity sensing, Context sensing, Physiological state sensing
Humistor	Detects humidity	Activity sensing
Infra-red camera	Infra-red frequency of light	Activity sensing, Context sensing
Radio frequency identification receiver	Radio frequency	Context sensing
Sonar	Detect objects through sound waves	Activity sensing
Software Sensors	Detect user's actions	Context sensing
WiFi	Radio frequency	Context sensing

2.3 FACTORS TO CONSIDER IN CHOOSING A SENSOR

Factors to consider in making the right choice of sensors for your specific circumstances include the following:

Geometry – The sensor needs to be the appropriate shape and size to fit your needs.
Measurement range – The sensor needs to be built to handle the appropriate range of measurement, whether it's temperature, pressure, flow, humidity, or another measurement.

Connectivity – The sensor needs to be able to easily connect to data loggers and other data acquisition and control equipment.
Deployment Environment - When implementing a wireless sensor system, understand the deployment environment to determine the topology of your network, the geographical location of measurement nodes,
Software and Data Access - A final factor to consider when implementing a wireless sensor is the software to be used to collect, analyse and present measurement data to local or remote clients.

2.4 Wireless Sensors Security Requirements

Many sensor networks are have mission-critical tasks to accomplish, hence there is a need to consider the security requirements at design stages. According to Bokare et al (2012) security requirements for any sensor architecture should include the following:

• *Authentication:* Since sensors use a shared wireless communication medium, authentication is necessary to enable sensor nodes to detect maliciously injected or spoofed packets. Authentication enables a node to verify the origin of a packet (source authentication) and ensure data integrity, that is, ensure that data is unchanged (data authentication).

• *Secrecy*: Ensuring the secrecy of sensed data is important for protecting data from eavesdroppers. Standard encryption functions can be used to achieve secrecy.

• *Countermeasures*: Standard cryptographic techniques can protect the secrecy and authenticity of communication links from outsider attacks such as eavesdropping, packet replay attacks, and modification or spoofing of packets.

• *Key Establishment*: for two sensor nodes to set up a secret and authenticated link, they need to establish a shared secret key.

• *Broadcast Authentication*: in broadcast source authentication, possible approach is to use a digital signature, where the source signs each message with a private key and all the receivers verify the message using the public key.

2.5 CHALLENGES WITH WIRELESS SENSORS

Despite the advancements and the breakthrough experienced with wireless sensors, major issues still plague the design and performance of wireless sensors. Below are some of the challenges:

2.5.1 Energy: Sensors require power for various operations. Energy is consumed in data collection, data processing, and data communication; also, continuous listening to the medium for faithful operation demands a large amount of energy by node components (CPU, radio, etc.) even if they are idle.

Batteries providing power need to be changed or recharged after they have been consumed. Sometimes it becomes difficult to recharge or change the batteries because of demographic conditions.

2.5.2 Self-Management: Wireless sensors once deployed should be able to work without any human intervention. It should be able to manage the network configuration, adaptation, maintenance, and repair by itself. This is rarely achievable as physical management of the nodes are required to ensure they are properly positioned and capturing the correct data

2.5.3 Operating System: Operating System for Wireless Sensors should be less complex than the general operating systems and should have an easy programming paradigm.

2.5.4 Quality of Service (QoS): Wireless sensors are being used in various real time and critical applications, so it is mandatory for the wireless sensor to provide good QoS. Though, it is difficult because the network topology may change constantly and the available state information for routing is inherently imprecise.

2.5.5 Security: Confidentiality is required in sensor networks to protect information traveling between the sensor nodes of the network or between the sensors and the base station; otherwise it may result in eavesdropping on the communication.

2.5.6 Data Collection and Transmission: Data gathering is the main objective of sensor nodes. The sensors periodically sense the data from the surrounding environment, process it and transmit it to the base station or sink. Sometimes the sample of data collected is redundant and there is no need of transmitting such samples to the sink node as it will only consume energy. So care must be taken during data collection and transmission.

3. HUMAN COMPUTER INTERACTION (HCI)

Human computer Interaction (HCI) is defined as a discipline concerned with the design, evaluation and implementation of interactive computing systems for human use and with the study of major phenomena surrounding them (Hewett et al, 1996).

HCI has long been a focal area for innovative, multidisciplinary computing research and development. (Carroll, 2002). HCI consists of three parts: the user, the computer itself, and the ways they work together (Preece, 1994):

The goals of HCI are to produce usable and safe systems, as well as functional systems. These goals can be summarized as 'to develop or improve the safety, utility, effectiveness, efficiency and usability of systems that include computers'. Human Computer Interaction must also improve the interactions between users and computers by making computers more operational and receptive to the user's wants. Finally, HCI must develops or improves certain goals in designing devices.

3.1 STRUCTURE AND SCOPE OF HCI

HCI, as the name suggests, comprises three major parts within the framework: the user, the computer, and the interaction, indicates the ways they work together to achieve goals. Figure 2 below shows three main components of human computer interaction.

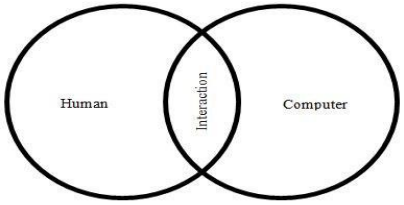

Figure 2: HCI Components

Human-Computer Interaction studies how people design, implement and use computer interfaces (Hollan, 2003). HCI has become an umbrella term for a number of disciplines including theories of education, psychology, collaboration as well as efficiency and ergonomics (Hinze-Hoare, 2007).

3.2 HCI AND USER ACTIVITY INTERACTION LEVELS

The field of HCI continues undergoing fast changes with the development of new multi-sensory user interface and metaphors. Smart devices, information processing engine, and large interactive displays have become more permeate (Gouin & Lavigne, 2010). It has been widely accepted that the user activity has three interaction levels: physical, cognitive, and affective.

3.2.1 Physical

Te'eni et al (2007) in their book pointed out that the physical aspect combines the study of human body mechanics and physical limitations with industrial psychology to reach a fit between human and computer and accordingly improving the performance and the user's well-being.

.Moreover, the existing physical technologies for HCI generally can be organized by input and output devices. Input devices are the most obvious interactive technologies. These devices are generally organized around the human senses including vision, audition, and touch.

3.2.1.1 Vision. Vision is an important aspect in computer usage. It is the human process of seeing and comprehending objectives (Te'eni et al., 2007). For example, the size of the characters, the color of the foreground and background on the screen, and the angle and brightness of screen are all aspects of vision that may affect the interaction between users and computers.

3.2.1.2 Audition. The sense of hearing also plays an important role in human performance. Speech recognition is generally considered as the ability of computer to recognize

human speech, usually with an audition device. Those difficult-to-build devices require advanced technologies to narrow the gap between human and computer. Alarms, beeps, and turn-by-turn navigation commands of a GPS device are common examples (Karray et al, 2008).

3.2.1.3 Touch. The sense of touch helps human beings understand the world at large. Touch is extremely important for the visually impaired. The keyboard and other direct manipulation devices such as the mouse have some relation to touch (Te'eni et al., 2007).

3.2.2 Cognitive

The cognitive aspect of interaction deals with ways of human understanding and interacting with computer systems. Cognitive engineering is a discipline that applies the combined knowledge of cognitive psychology and information technology to the design of artifacts. It aims to reduce complexity of interaction (Te'eni et al., 2007).

3.2.3 Affective

Affective refers to psychological processes and states including feelings, emotions, attitudes, satisfaction, and impressions. The affective aspect of interaction attempts to make the interaction with a cheerful experience and to affect the user to continue using the machine by changing their attitudes and emotions.

3.4 HCI Modality

An interface mainly relies on number and diversity of its inputs and outputs which are communication channels that enable users to interact with computer via this interface. Each of the different independent single channels is called a modality [Jaimes et al, 2007]. A system that is based on only one modality is called unimodal. Based on the nature of different modalities, they can be divided into three categories:

- *Visual based:* This include facial expression analysis, body movement tracking, gesture recognition, gaze detection (eye movement tracking).
- *Audio based*: This include speech recognition, speaker recognition, auditory emotion analysis, human-made noise detections (gasp, sigh, laugh, cry, etc) and musical interaction.
- *Sensor based*: The commonality of these areas is that at least one physical sensor is used between user and machine to provide the interaction. These include: Pen-based interaction, mouse & keyboard, Joysticks, Motion tracking sensors and digitizers, haptic sensors, pressure sensors, taste/smell sensors

3.5 Multimodal HCI Systems

Multimodal is combination of multiple modalities. The modalities mostly refer to the ways that the system responds to the inputs or the communication channels. Multimodal interface acts as a facilitator of human-computer interaction through two or more nodes of input. It is expected that multimodal HCI system is combination of single modalities that interact correlatively.

An interesting aspect of multimodality is the collaboration of different modalities to assist the recognitions. For example, lip movement tracking (visual-based) can help speech recognition methods (audio-based) and speech recognition methods (audio-based) can assist command acquisition in gesture recognition (visual-based). Examples of applications of multimodal systems are: Smart Video Conferencing, Intelligent Homes/Offices, Driver Monitoring, Intelligent Games and applications for helping people with disabilities.

4. REVIEW OF RELATED WORKS

Bhagwani, Sengar & Talwaniper (2012) developed a model Brain Computer Interface (BCI) tending toward the development of a device that can be controlled by thoughts, such as ability to change channels with mind or thought by capturing brain signals and translating them into commands that allow humans to control (just by thinking) devices such as computers, robots, rehabilitation technology and virtual reality environments. BCIs are often aimed at assisting, augmenting, or repairing human cognitive or sensory-motor functions**.**

Venkata and Neelima (2014) developed a tilt sensor computer controlled mouse which consist of an economical head operated computer mouse for people with disabilities as shown in figure 3. It focuses on the invention of a head operated computer mouse that employs one tilt sensor placed in the headset to determine head position and to function as simple head-operated computer mouse. The system uses accelerometer based tilt sensor to detect the user's head tilt in order to direct the mouse movement on the computer screen. Clicking of mouse is activated by the user's eye brow movement through a sensor. The keyboard function is designed to allow the user to scroll letters with head tilt and with eye brow movement as the selection mechanism. Voice recognition section is also present in the head section to identify the small letters which are pronounced by the paralyzed user.

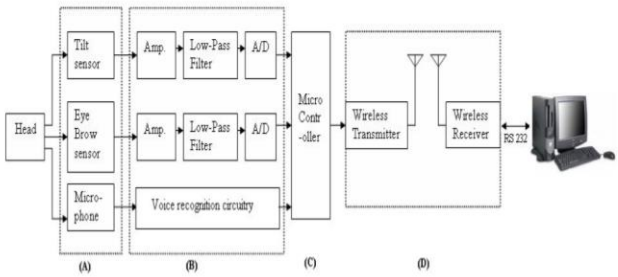

Figure.3. Block diagram representation of the tilt sensors-controlled computer mouse interface.
Source: Venkata and Neelima 2014

Rajangam, Tseng, Yin, Lehew, Schwartz, Lebedev, and Nicolelis (2016) showed that rhesus monkeys can learn to navigate a robotic wheelchair, using their cortical activity as the main control signal. Two monkeys were chronically implanted with multichannel microelectrode arrays that allowed wireless recordings from ensembles of premotor and sensorimotor cortical neurons. Initially, while monkeys remained seated in the robotic wheelchair, passive navigation was employed to train a linear decoder to extract 2-Dimesionl wheelchair kinematics from cortical activity. Next, the monkeys were able to translate their cortical activity into the robotic wheelchair's translational and rotational velocities. Over time, monkeys improved their ability to navigate the wheelchair toward the location of a grape reward. These can be used to restore whole-body mobility to severely paralyzed patients in the future.

Chen, Xue, Mei & Oetomo (2016) presented a state-of-art of wearable system for infant movement monitoring. The system showed how Neonatologist can give appropriate treatment and provide optimal nursing condition through the aid of wearable sensor. This is done by using sensor to monitor the body movement in infants as shown in figure 4

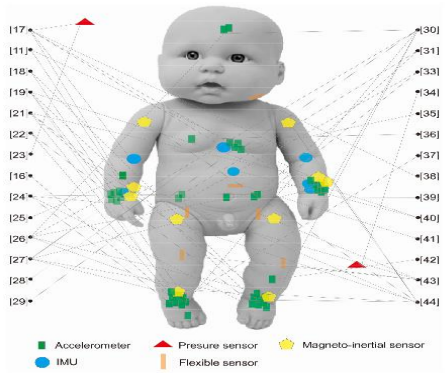

Figure 4: Infographic of sensor placement (Chen, Xue, Mei & Oetomo 2016)

(Prange, Chikobava, Poller, Barz, & Sonntag (2017) designed an interactive, real-time decision support for medical domain where physician and patient interact in virtual reality environment by using natural speech and hand gestures. The system involve the use of mobile tablet with stylus by radiologist to transcribe data in real-time using automated handwritten recognition, parsed, and representation based on medical ontologies. It creates a fully digital version of the radiology findings (mammography). The system is with a highly flexible architecture which can be connected to the existing hospital database systems (e.g, a picture archiving and communication system) and connects interaction devices such as Virtual Reality glasses and head-mounted displays.

Sandeep Kumar Singh et al (2018) investigated an animal-human cohabitation problem with the help of machine learning and fibre-wireless access networks integrating cloud and edge computing, and then proposed an early warning system which detects wild animals nearby road/rail with the help of wireless sensors and alerts passing vehicles of possible animal crossing.

5. HCI AND HUMAN ABILITIES

The growing importance of human computer interaction (HCI) is a result of the widespread deployment of computers connecting with humans. The enhancement of human senses electronically is possible when pervasive computers interact unnoticeably with humans in ubiquitous computing.
Ubiquitous Computing regarded as ''The Computer for The 21st Century'' even envisioned future computers to be invisibly living with humans, thereby widening the range of user types. With the popularity of the internet in recent decades, the concept of internet of things (IoT) further boosts the applications of ubiquitous computing to connect almost everything electronic to the Internet, with the ultimate result for an unprecedented demand for better HCI technology to cope with the needs for the huge number of non-technical users interacting with billions of network-connected computers.

5.1 Natural user interface (NUI) Versus Disappearing User Interface (DUI)

Human computer interaction is a multidisciplinary technology that heavily focuses on human-centric user interface design. An emerging trend in HCI is the design of Natural user interface (NUI) where humans can interact naturally with computers instead of using conventional methods such as command line interface (CLI) or graphical user interface (GUI), NUIs have been criticised as being ''artificial naturallity'' and as not representing natural human behaviours especially gesture based interactions (Malizia and Bellucci 2012) Hence, the introduction of the Disappearing User Interface (DUI) as a logical provision of natural HCI. DUI are tangible and intangible user interfaces that exist and work well but are not noticeable by humans, and are classified into three main categories:

- Human Body as DUIs
- Edible and Implantable DUIs
- Wearable DUIs

DUI is a natural HCI focusing on interaction with the contents instead of the interfaces (Lim 2012). Humans are content receivers through the sensory systems, and at the same time humans are content providers mainly through muscular movements and nervous systems. DUIs enable the conveyance of contents between humans and machines in a natural way through tangible or intangible artefacts; touch or touchless interface; outside or inside human bodies; and most importantly not noticeable by the target persons so the interaction is done based on intuition. DUI is multi-modal in nature by sensing human behaviours through different disappearing user interfaces in a natural way and creating the contents for exchange.
DUIs may interact with human inputs mainly through the five basic senses: vision, hearing, touch, smell and taste.
Humans do have more than five senses and they all fall into the same ''stimulus-sensation-perception'' process with the human brain as the final decision maker after interpreting the outside world from the stimuli.

Figure 5 shows a typical illustration of a human sensory system and it can be seen that human perception based on the human brain is the result of decoding the sensation signals which are activated by the stimuli coming from the outside world through the basic sensory organs, while human outputs are the responses to this perception.

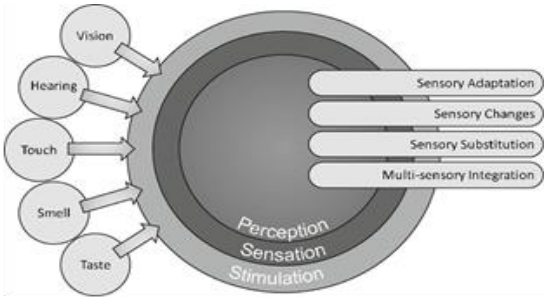

Figure 5: The Human Senses

Hearing is another popular human input interface, while computer generated sound in the audio frequency range is delivered through a medium to the human auditory system. Sonic interface is a good DUI for naturally interfacing with humans in open space, and the critical requirement is the delivering of high quality sound signals which can normally be achieved through frequency response equalisation. The sense of touch also enables a private communication with computers through the human skin.

Human smell, which is a chemical sense is another human input interface. Presentation of smell stimuli can be achieved through diffusion to open air but the vaporisation of odour molecules is relatively slow compared to the propagation of mechanical waves in sound and electromagnetic waves in vision, thus a continuous emission of odour vapour is normally applied.

Despite that the nature of stimulus to each type of sense organ is different, the perception can be the same. Sensory Substitution is an emerging research demonstrating that Brain Plasticity enables human brain to choose a particular type of sensor or combination of sensors to arrive at the same perception after a training period (Bermejo and Arias 2015). DUI should therefore be more effective to interface with human inputs through delivering content instead of raw data, and the more we know about the human brain, the more we will realise how to interface with humans.

DUIs also capture human outputs based on monitoring human body activities: body parts movements, body sound generation, body temperature variations, body odour emissions, and the dynamic physiological parameters. The disappearing nature of DUI avoids step-by-step manual driven human interaction, and its focus is set on interfacing with the contents which are the actions generally derived from human perceptions (Lim 2012).

6. IMPROVEMENT OF HUMAN ABILITY WITH HCI

For many years, humans have sent commands to "machines" primarily via the keyboard-mouse paradigm also known as WIMP (windows, icons, menus, point-and-click devices). Here, the term *machine* is used in a very broad sense: in addition to the point-and-click devices that are usually associated with computers, a keyboard of sorts is used to dial numbers on a telephone, to interact with a TV, to select a wide range of functions on a car dashboard, and many other activities that employ key-based interaction modalities. In most cases, the machine's output to the user is then based on a display device such as a monitor.

As foreseen by Andy van Dam, in his vision paper published in IEEE Computer Graphics & Applications' first issue of the new century: "Post-WIMP interfaces will not only take advantage of more of our senses but also be increasingly based on the way we naturally interact with our environment and with other humans."

Several affordable sensors have begun to shake up the way people interact with devices. Touch and multi-touch screens have driven the change from cellular phones to smartphones, and gestures are now the main interaction modality to activate functions on personal devices. At the same time, speech recognition technologies and CPUs' increased computational power now let users efficiently provide inputs when they can't perform gestures.

Personal devices are the most evident example of how new forms of HCI can reduce the gap between humans' mental models and technology. One market that has led this deep innovation in HCI is entertainment. With users asking game and device makers for new ways to control characters, game console developers proposed controllers to release players from the constraints of using a keyboard and a mouse. The new interface becomes a means for providing tactile feedback as well as acting as a sort of tangible interface (the controller becomes a steering wheel, a gun, or a tennis racket).

Sensors such as the Microsoft Kinect are a further step toward the implementation of fully natural interfaces in which the human body becomes the controller. The device lets users provide commands to the machine via gestures and body poses as embedded hardware performs real-time processing of raw data from a depth camera, thus obtaining a schematic of a human skeleton comprising a set of bones and joints. Recognizing the position and orientation of bones lets the hardware identify poses and gestures, which can be mapped to commands for the machine.

Researchers have also proposed sensors that can track a user's hands. For instance, the Leap Motion can interactively track both hands of a user by identifying the positions of finger tips and the palm centre. Some car makers are already proposing a hand-tracking based alternative interaction modality in lieu of traditional touch screens devoted to managing infotainment functions. Similarly, some smart Televisions let users control their choices with a set of gestures, thus replacing the traditional remote control.

Found only in science fiction movies just a few years ago, the above-mentioned scenarios are now the present reality of HCI. On the other hand, new and more intriguing scenarios appear to be imminent, as brain interfaces seem poised to invert the relationship between humans and machines, for instance. This new interaction paradigm's success will rely on future technological advances, which aim to transform interface devices into wearable and embeddable objects.

Interfaces based on augmented reality (AR) technologies are clear examples of this transformation. Many applications for tourism, entertainment, maintenance, shopping, and social networks are already available for personal devices, but new wearable sensors might soon change our habits.
Eye-tracking is also replacing tasks usually performed by the mouse. Eye-tracking can help in picking up the cues that are subconsciously given by the other person and hence, in enhancing the overall interaction Eyes can reveal a lot about a person's intentions, thoughts and actions, as they are good indicators of what we're interested in. There's a lot of potential in eye-tracking in other arenas as well.
Wearables, the Internet of Things and Smart Materials are realms that are opening ways for even more eccentric and unimaginable things, into a future with great improvement on human abilities with HCI

7. CONCLUSION

This paper reviewed the applications of sensors in HCI, how integrating sensors with human ability enhances the possibilities of HCI and what can be done. HCI can be implemented virtually in all spheres of life and offer opportunities to make life comfortable and enjoyable. New forms of HCI with the use of wireless sensors will change our lives significantly and improve the quality of life of people who cannot take advantage of current interfaces due to physical disabilities. The opportunities for HCI are tremendous with progress made toward more user-friendly and natural interfaces for human-machine interaction. Finally, further research on the integration of sensors with HCI will help to solve many problems in future.

8. FUTURE OF HCI

The future of HCI is anchored on multimodality, intelligent, adaptive interfaces and active interfaces. Multi-modal interfaces attempt to address the problems associated with purely auditory and purely visual interfaces by providing a more immersive environment for human-computer interaction.
The interfaces of the future should be Non-Windows, Icons, Menus, Pointer (Non-WIMP) and more of natural features than artificial**.** HCI must give special attention for language understanding, mobile and handheld Interaction for rich user experience and high level of functionality.
HCI must think beyond audiovisual Interfaces by providing new tools for interactive experience design and also help to uncover sensory stimulation and emotional responses that can be used in the future for better human computer interaction. There is still a lot of challenge in understanding people's multisensory experiences in HCI because the senses we call upon when interacting with technology are restricted. Another future goal is to understand the ways in which our senses process information and how they relate to one another to create richer experiences for human-technology interactions.

9. ACKNOWLEDGMENTS

Our thanks to the current and previous students of Human Computer Interaction and Sensors Research group of the Computer Science Department of the School of Computing and Engineering Sciences, Babcock University, Ilishan-Remo, Nigeria who have contributed towards the development of this paper.

10. REFERENCES

1) Bermejo F, Di Paolo EA, Hüg MX and. Arias C, Sensorimotor strategies for recognizing geometrical. shapes: a comparative study with. different sensory substitution devices : *Frontiers in Psychology 6* , **2015** DOI: 10.3389/fpsyg.2015.00679

2) Bhagwani, A, Sengar, C and Talwaniper, J (2012). Human Computer Interaction. International Journal of Advancements in Research & Technology Vol 1 Issue 3 pp 72-76

3) Bokare, M and Ralegaonkar, A (2012). Wireless Sensor Network: A Promising Approach for Distributed Sensing Tasks; Excel Journal of Engineering Technology and Management Science, Vol. I No.1; ISSN 2249-9032

4) Carroll., J (2002)."Human-Computer Interaction in the New Millenium," ISBN-13: 978-0-201-70447-1

5) Chen, H; Xue, M;Mei, Z; Bambang Oetomo, S; Chen, W (/2016). A review of wearable sensor systems for monitoring body movements of neonates. Sensors 2016, 16,2134;doi : 10.3390/s/16122134 www.mdpi.com/journal/sensors

6) Dargie, W, Poellabauer,C (2010). Fundamentals of wireless sensor networks: theory and practice. John Wiley & Sons.

7) Fraden J, 2016: Handbook of Modern Sensors, Available at: https://doi.org/10.1007/978/3/319/19303/8/1

8) Fritzsche, B. (2015). Human Computer Interaction in the Internet of Things Era. Munich: University of Munich Department of Computer Science Media Informatics Group.

9) Gouin, D. & Lavigne, V. (2010). Trends in human-computer interaction to support future Intelligence analysis capabilities. Paper presented at the Sixteenth International Command and Control Research and Technology Symposium, Quebec City, Canada.

10) Hewett, Baecker, Card, Carey, Gasen, Mantei, Perlman, Strong and Verplank, "ACM SIGCHI Curricula for Human-Computer Interaction," 1996. http://old.sigchi.org/cdg/cdg2.html

11) Hinze-Hoare, V. (2007). "Review and Analysis of Human Computer Interaction (HCI) Principles", Southampton University, pp.2

12) Hollan, J. D. (2003). Human-Computer Interaction",The MIT Encyclopedia of the Cognitive Sciences, Robert Wilson and Frank Keil (Eds), MIT Press, San Diego, pp.1

13) Hua, K, Yea, J, Fana, E, Shena, S, Huanga, L, Pi, J (2017). A novel object tracking algorithm by fusing color and depth information based on single valued neutrosophic cross-entropy. Journal of Intelligent & Fuzzy Systems (32), 1775-1786.

14) Jaimes, A and Sebe, N 2007 "Multimodal human computer interaction: a survey", Computer Vision and Image Understanding, 108(1-2), pp 116-134.

15) Kalantar-zadeh (2013). Sensors: An Introductory Course 2013 Edition, Kindle Edition. by Kourosh Kalantar-zadeh ebook . *Available at* https://www.amazon.com/Sensors-Introductory...Kalantar-zadeh.../B00C6BZROU

16) Karray, F., Alemzadeh, M., Saleh, J. A., & Arab, M. N. (2008). Human-computer interaction: overview on state of the art. *International Journal on Smart Sensing and Intelligent Systems, 1*(1), Pp. 137-159.

17) Lim YK (2012) Disappearing interfaces. Interactions 19(5):36–39. doi:10.1145/2334184.2334194

18) Malizia and Bellucci 2012; The Artificiality of Natural User Interfaces: Communications of the ACM 55(3):36-38 · March 2012 *https://dl.acm.org/citation.cfm?id=2093563*

19) Paravati, G. Gatteschi, V, (2015). Human-Computer Interaction in Smart Environments. *Sensors, 15*, 19487-19494.

20) Prange, A, Chikobava, M, Poller, P, Barz, M, Sonntag, D (2017). A Multimodal Dialogue System for Medical Decision Support in Virtual Reality. Proceedings of the SIGNAL, Conference, pages 23-26. Association for Computational Linguistics.

21) Preece, J. (1994), "Human Computer Interaction", Addison Wesley pp.6, 26

22) Rajangam, Tseng, Yin, Lehew, Schwartz, Lebedev, and Nicolelis (2016): Wireless Cortical Brain-Machine Interface for Whole-Body Navigation in Primates. National Center for Biotechnology Information, U.S. National Library of Medicine. Available at https://www.ncbi.nlm.nih.gov/pubmed/26938468

23) Sandeep Kumar Singh et al (2018): Improving Animal-Human Cohabitation with Machine Learning. Available at: https://www.mdpi.com/2224-2708/7/3/35/pdf

24) Spencer F., Manuel E., & Narito K., (2014) Smart Sensing Technology: Opportunities and Challenges. Structural Control and Health Monitoring 11(4):349 - 368 *Available at* https://www.researchgate.net/.../227533576_Smart_Sensing_Technology_Opportunities

25) Sunny, George and Kizhakkethottam, (2015): Applications and Challenges of Human Activity Recognition Using Sensors In A Smart Environment: International Journal for Innovative Research in Science & Technology. Volume 2 Issue – 4

26) Te'eni, D., Carey, J., & Zhang, P., (2007). Human computer interaction developing effective organizational information systems. Hoboken John Wiley & Sons,

27) Varkey, J., Pompili, D., & Walls, T. (2012). Human motion recognition using a wireless sensor-based wearable system. *Personal & Ubiquitous Computing, 16*(7), 897-910.

28) Venkata, M and Neelima, B. 2014:A Portable Wireless Head Movement Controlled Human-Computer Interface for People with Disabilities International Journal of Advanced Research in Electrical, Electronics and Instrumentation Engineering (An ISO 3297: 2007 Certified Organization) Vol. 3, Issue 7, July 2014